Supplementary Information

Viscosity Effects on the Chemiluminescence Emission of 1,2-Dioxetanes in Water

Maidileyvis Castro Cabello[a], Palanisamy Kandhan,[a] Peng Tao[a] and Alexander R. Lippert[a*]

[a]Department of Chemistry, Southern Methodist University, Dallas, Texas 75275-0314

*Corresponding author e-mail: alippert@mail.smu.edu (Alexander R. Lippert)

Contents

General Synthetic Materials and Methods

Reagents were purchased from Sigma-Aldrich (St. Louis, MO), Thermo Fisher Scientific (Waltham, MA), TCI America (Portland, OR), Alfa Aesar (Ward Hill, MA), EMD Millipore (Billerica, MA), Oakwood Chemical (West Columbia, SC), or Cayman Chemical (Ann Arbor, MI) and used without further purification. ^{1}H NMR and ^{13}C NMR were obtained on a JEOL 500 MHz spectrometer in $CDCl_3$ (Cambridge Isotope Laboratories, Cambridge, MA). All chemical shifts are reported in the standard notation of parts per million. Splitting patterns are indicated as follows: s, singlet; d, doublet; t, triplet; q, quartet; m, multiplet; dd, doublet of doublets; bs, broad singlet. Low resolution mass spectroscopy was performed on a Advion LCMS (ESI source). Safety risks for synthetic organic chemistry related to exposure to hazardous materials were mitigated by using fume hoods, lab coats, safety goggles, and gloves. While we have never had an incident, dioxetanes are high energy compounds that pose a risk of explosion. Dioxetanes are typically prepared on scales smaller than 100 mg to mitigate explosion risks.

Viscosity measurements

Viscosities of the PBS and their mixtures with PEG-3350 or ethylene glycol were measured using an Ostwald capillary viscometer[1] (Table S1 and S4).

Fluorescence measurements

Absolute fluorescence quantum yields (Φ_{FL}) of the ester decomposition products were measured in HORIBA QM8075-11-C spectrophotometer using an integrating sphere (Table S2).

Empirical polarity parameter

The medium polarity parameter $E_T(30)$ of the mixtures were determined at 25.0 °C, with Reichardt's pyridinium-*N*-phenolate betaine dye, as described elsewhere[2]. Briefly, a stock solution of Reichardt's dye was prepared in acetone (1.8 10^{-3} mol L^{-1}) and 20 µL of this solution was added to glass tubes and the acetone was evaporated. The solutions of the PBS and their mixtures with PEG-3350 or ethylene glycol contained 1.33% of DMSO were added to the tubes. The final probe concentration in the solutions was 1.2 10^{-4} mol L^{-1}. UV-VIS spectra were obtained and using the maximum absorbance wavelength values (λ_{max}) (from the probe's intramolecular charge transfer band), the empirical polarity value is calculated, based on the $E_T(30)$ scale (Eq. S1, Table S3)

$$E_T(30),\ \text{kcal/mol} = 28591.5/\ \lambda_{máx}\ (\text{nm}) \qquad \text{(Eq. S1)}$$

Kinetics of the decomposition of acrylonitrile 1,2-dioxetane

A stock solution of 1,2-dioxetanes in DMSO (4 µL) was added by using a microsyringe to the different mixtures (296 µL) contained in the quartz cell placed in the thermostated cell holder of the HORIBA QM8075-11-C spectrophotometer. Each experiment was independently conducted in triplicate at 25 °C. The observed rate constants (k_{obs}) were obtained by fitting the intensity versus time curves using a mono exponential decay function (Eq S2., Figures S2, S3).

$$I = I_0 + A_1 e^{-k_{obs}\, t} \qquad (Eq.\ S2)$$

Chemiluminescence Quantum Yields (Φ_{CL})

The singlet quantum yields (Φ_s) were determined using Eq S3 where Φ_{CL} is the CL quantum yield calculated using a variation of the methodology previously reported with a luminol calibration standard[3,4] and Φ_{Fl} is the fluorescence quantum yields of the emitter species. Eq S4 summarizes calculation of Φ_{CL}: Q_{diox} is the total light emission from dioxetanes, obtained by integrating the corresponding kinetic profiles, n_{diox} is the number of moles of dioxetanes, f_{lum} is the calibration factor to convert the total light emission of the sample from arbitrary units to Einstein units, calculated using the chemiluminescent standard luminol, Φ_{lum} is the reference chemiluminescence quantum yield of luminol (0.0114 ± 0.0006 E mol^{-1}), Q_{lum} is the integrated emission intensity under a kinetic emission profile of luminol in PBS at pH 11.6 with consecutive additions of hemin, and n_{lum} is the number of moles of luminol used, F_{spect} is the spectral correction factor, calculated as the light that passes through the wavelength selective monochromator at a particular wavelength (integrated intensity from [λ − ½ slits] to [λ + ½ slits]) as a fraction of the total light emission of the sample across all wavelengths (integrated intensity from 400 to 800 nm) (Equation S5). This accounts for the differences in spectral shape between luminol emission and dioxetanes emission. $F_{spect(lum)}$ was calculated using luminol emission spectrum, and $F_{spect(diox)}$ with dioxetanes emission spectrum (Eq S6). To account for the sensitivity of the photomultiplier tube detector at different wavelengths, we enabled real-time corrections

on the instrument which automatically correct the raw data based on the manufacturer provided correction factors at each wavelength. These corrected traces were used in all calculations.

$$\phi_S = \frac{\Phi_{CL}}{\Phi_{Fl}} \qquad (Eq\ S3)$$

$$\phi_{CL} = \frac{Q_{diox} f_{lum} F_{spect(lum)}}{n_{diox} F_{spect(diox)}} \quad (Eq\ S4)$$

$$f_{lum} = \frac{\phi_{lum} n_{lum}}{Q_{lum}} \qquad (Eq\ S5)$$

$$F_{spect} = \frac{\int_{\lambda - slit/2}^{\lambda + slit/2} S(\lambda) d\lambda}{\int_{\lambda_i}^{\lambda_f} S(\lambda) d\lambda} \quad (Eq\ S6)$$

Table S1. Viscosity values of different mixtures of PBS/PEG-3350 and PBS/EG, at 25 °C.

	Viscosity (cP)	
Weight %	**PEG-3350**	**EG**
0	0.89	0.89
5	1.58	1.11
15	4.32	1.47
30	10.16	2.15

Table S2. Fluorescence quantum yields (Φ_{FL}) of the authentic emitter at different mixtures of PBS/PEG-3350 and PBS/EG.

	Φ_{FL}			
	Monocyclic Dioxetane		**Bicyclic Dioxetane**	
Weight %	**PEG-3350**	**EG**	**PEG-3350**	**EG**
0	0.440 ± 0.001	0.440 ± 0.001	0.514 ± 0.009	0.514 ± 0.009
5	0.500 ± 0.004	0.46 ± 0.001	0.533 ± 0.007	0.51 ± 0.01
15	0.54 ± 0.01	0.504 ± 0.004	0.512 ± 0.01	0.503 ± 0.007
30	0.581 ± 0.004	0.517 ± 0.005	0.52 ± 0.01	0.505 ± 0.001

[PBS] = 100 mM, 1.3 % DMSO, pH = 7.4, 25 °C

Table S3. Solvent polarity parameter ($E_T(30)$) of different mixtures of PBS/PEG-3350 and PBS/EG, at 25 °C.

	$E_T(30)$ (kcal/mol)	
Weight %	**PEG-3350**	**EG**
0	93.74	93.74
5	93.13	93.74
15	92.53	93.74

30	91.93	93.43

Table S4. Viscosity values of different mixtures of PBS/PEG-3350 at 25–60 °C.

	Viscosity (cP)				
Weight %	**25 °C**	**30 °C**	**40 °C**	**50 °C**	**60 °C**
0	0.89	0.79	0.66	0.56	0.49
5	1.58	1.36	1.05	0.85	0.71
15	4.32	3.73	2.87	2.28	1.87
30	10.16	8.47	6.12	4.62	3.61

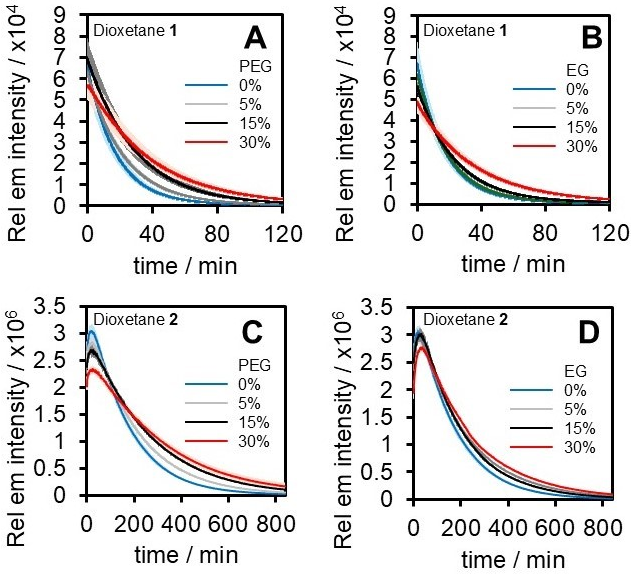

Figure S1. Average kinetic emission intensity profiles for the decomposition of (**A**) 0.66 μM **1** and (**B**) 10 μM **2** in different mixtures of PBS/PEG-3350, and (**C**) 0.66 μM **1** and (**D**) 10 μM **2** in different mixtures of PBS/EG (ethylene glycol). This is the same data as found in the manuscript Figure 1 with error bars included as ± S.D., n = 3 technical replicates.

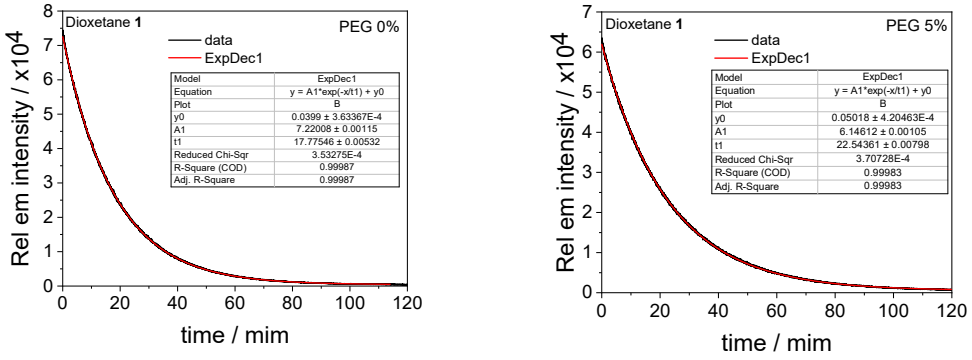

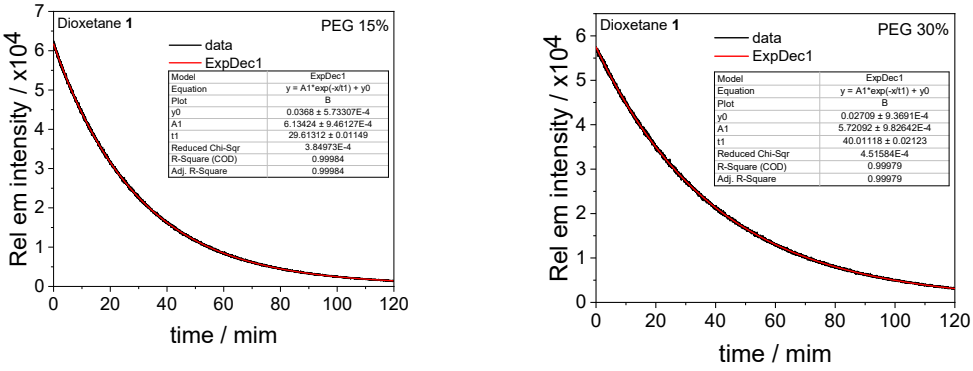

Figure S2. Representative kinetic fits for 0.66 μM dioxetane **1** in different mixtures of PBS/PEG-3350.

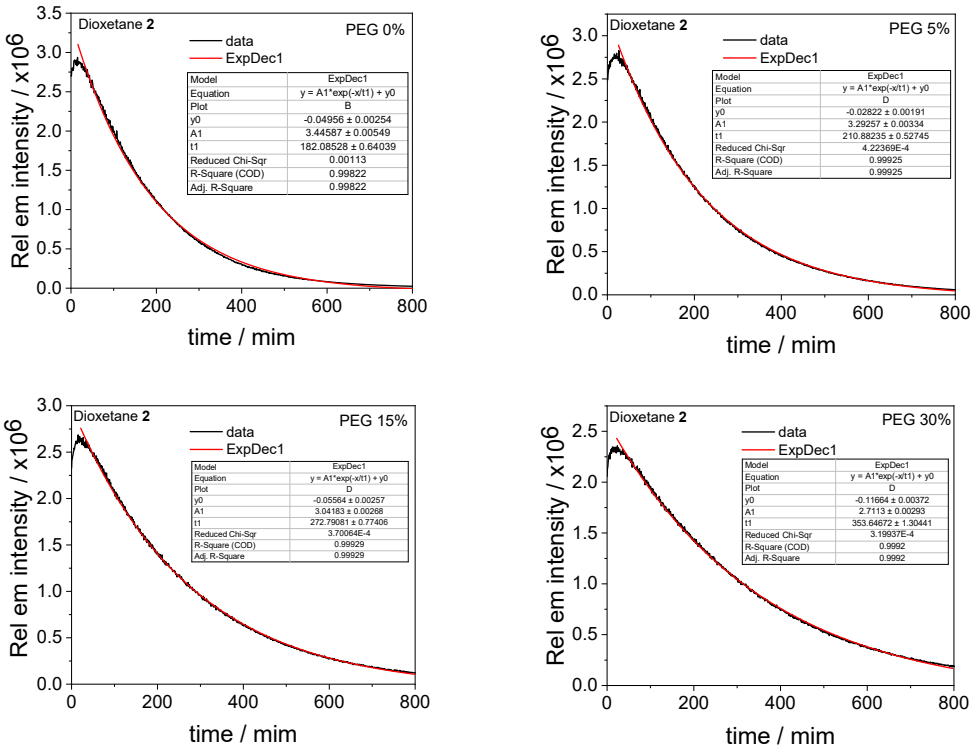

Figure S3. Representative kinetic fits for 10 μM dioxetane **2** in different mixtures of PBS/PEG-3350.

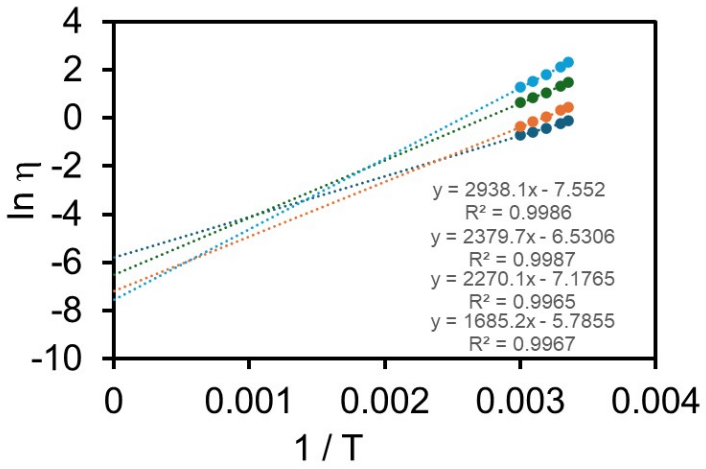

Figure S4. Arrhenius plots for the dependence of viscosity on temperature for aqueous solutions containing 0% PEG-3350 (dark blue), 5% PEG-3350 (orange), 15% PEG-3350 (dark blue), and 30% PEG-3350 (light blue).

Synthetic Procedures

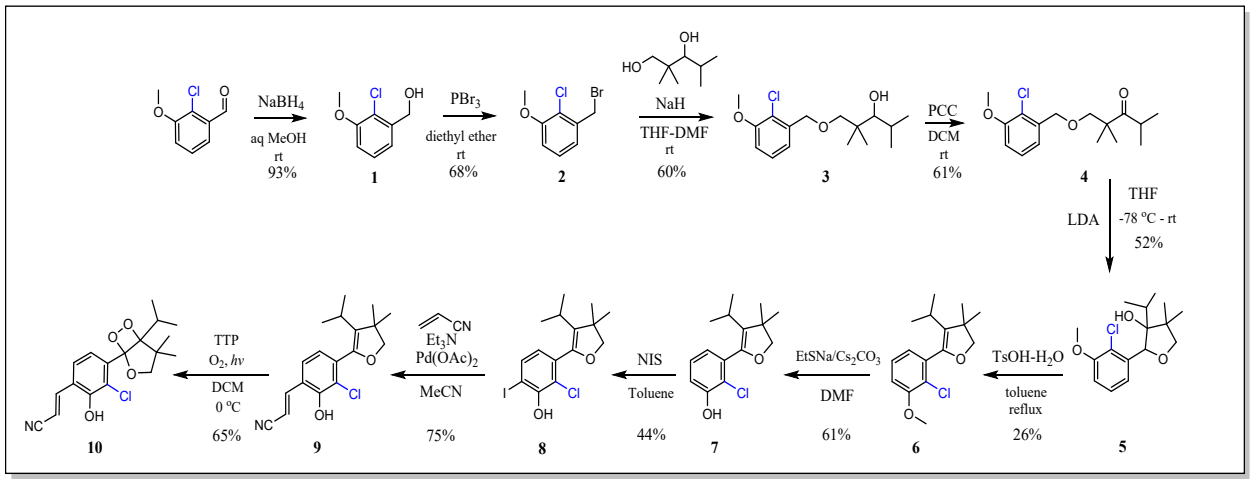

Scheme S1. Synthesis of bicyclic dioxetane **2**.

(2-chloro-3-methoxyphenyl)methanol **(1)** 2-chloro-3-methoxybenzaldehyde (15 g, 0.09 mol) was dissolved in 300 mL of methanol. A solution of sodium borohydride (5 g, 0.13 mol) in 150 mL of water was added dropwise at room temperature and stirred for 2 hours. Next, the mixture was acidified to pH 2 with 2M HCl and partly evaporated under reduced pressure. The aqueous residue was extracted with DCM, dried and evaporated giving compound **1** (14.45 g, 0.084 mol,

93 %) as a white solid. ^{1}H-NMR (500 MHz, $CDCl_3$): δ 3.90 (s, 3H), 4.78 (s, 2H), 6.88 (d, J= 8.6 Hz , 1H), 7.10 (d, J= 6.3, 1H), 7.23 (d, J= 8.05 , 1H) ppm. ^{13}C NMR (500 MHz, $CDCl_3$): δ 56.37, 63.14, 111.26, 120.50, 120.91, 139.87, 155.13 ppm.

1-(bromomethyl)-2-chloro-3-methoxybenzene **(2)** Compound **1** (2 g, 11.6 mmol) was dissolved in 50 mL of diethyl ether under nitrogen atmosphere. Phosphorus tribromide (15.08 mmol, 1.4 mL) was added to the solution at 0 °C. After stirred at room temperature for 12 hours, the solvent was evaporated and the residue was washed with water and extracted with ethyl acetate. After drying the solvent over sodium sulfate and removing it by rotary evaporation the crude product was then purified by chromatography on silica gel using DCM to afford compound **2** (1.86 g, 7.89 mmol, 68 %). ^{1}H-NMR (500 MHz, $CDCl_3$): δ 3.90 (s, 3H), 4.60 (s, 2H), 6.90 (dd, J= 8.6 and 1.7 Hz, 1H), 7.07 (dd, J= 8.0 and 1.7 Hz, 1H), 7.22 (t, J= 8.1 Hz, 1H) ppm. ^{13}C NMR (500 MHz, $CDCl_3$): δ 30.81, 56.44, 112.16, 122.94, 127.52, 136.91, 155.59 ppm. The ^{1}H-NMR is comparable with the previously reported spectrum in reference [5].

1-((2-chloro-3-methoxybenzyl)oxy)-2,2,4-trimethylpentan-3-ol **(3)** Sodium hydride (60 % in oil, 1.24 g, 31 mmol) was dissolved in a mixture of dry DMF:THF (1:1 v/v) (80 mL:80 mL) at 0 °C under nitrogen atmosphere. A solution of 2,2,4-trimethyl-1,3-pentanediol (3.4 g, 23.1 mmol) in dry THF (15 mL) was added dropwise over 5 min and stirred for 1 hour. After that, compound **2** (5 g, 21 mmol) was added to the solution and stirred for 3 hours at room temperature. The mixture was quenched with satd aq NH_4Cl and extracted with ethyl acetate. The organic layer was washed with brine, dried over Na_2SO_4 and concentrated. The crude was purified by chromatography on silica gel (2.5% EtOAc/Hexane) to afford the compound **3** (3.8 g, 12.6 mmol, 60 %) as a clear oil. ^{1}H-NMR (500 MHz, $CDCl_3$): δ 0.96 (m, 12 H), 1.88 (m, 1H), 3.32 (d, J= 8.6 Hz, 2H), 3.45 (d, J= 8.6 Hz, 1H), 3.88 (s, 3H), 4.57 (s, 2H), 6.87 (d, J = 7.4, 1H), 7.04 (d, J= 7.4, 1H), 7.21 (t, 1H) ppm. ^{13}C NMR (500 MHz, $CDCl_3$): δ 16.69, 20.89, 23.60, 23.60, 29.15, 39.34, 56.31, 70.80, 81.47, 82.30, 111.10, 120.59, 121.11, 127.25, 137.32, 155.06 ppm. HRMS calculated for $C_{16}H_{26}O_3Cl$ [M+H+] 301.1565, found 301.1578

1-((2-chloro-3-methoxybenzyl)oxy)-2,2,4-trimethylpentan-3-one **(4)** A suspension of Celite (2 g) and PCC (2 g, 10 mmol) was prepared in dry DCM (20 mL) at room temperature under nitrogen. A solution of compound **3** (2 g, 6.65 mmol) in dry DCM (5 mL) was added dropwise to a suspension and stirred for 12 hours. 2-propanol (5 mL) was added to the reaction and stirred for 30 minutes. After that, diethyl ether (200 mL) was added and the mixture was stirred for another 30 minutes. The reaction was filtered twice through Celite and concentrated. The product was purified by chromatography on silica gel (100 % DCM) to afford compound **4** (1.22 g, 4.1 mmol, 61 %). ^{1}H-NMR (500 MHz, $CDCl_3$): δ 1.02 (d, J = 6.3 Hz, 6 H), 1.19 (s, 6H), 3.1 (m, 1H), 3.57 (s, 2H), 3.89 (s, 3H), 4.57 (s, 2H), 6.85 (d, J = 7.4 Hz, 1H), 7.05 (d, J= 7.4 Hz, 1H), 7.21 (t, 1H) ppm. ^{13}C NMR (500 MHz, $CDCl_3$): δ 20.01, 21.84, 34.47, 49.24, 56.31, 70.44, 110.78, 120.31, 127.16, 137.76, 154.90, 218.88 ppm. HRMS calculated for $C_{16}H_{24}O_3Cl$ [M+H+] 299.1408, found 299.1417

2-(2-chloro-3-methoxyphenyl)-3-isopropyl-4,4-dimethyltetrahydrofuran-3-ol **(5)** Compound **4** (1 g, 3.35 mmol) was dissolved in 10 mL of dry THF under nitrogen. LDA (6.7 mL, 6.7 mmol) was

added dropwise at -78 °C and stirred at 0 °C for 3 hours. The solution was quenched with satd aq NH_4Cl and extracted with EtOAc. The organic layer was washed with brine, dried over Na_2SO_4 and concentrated. The residue was purified by chromatography on silica gel (5% EtOAc/Hexane) to afford compound **5** (0.52 g, 1.74 mmol, 52 %). ^{1}H-NMR (500 MHz, $CDCl_3$): δ 0.51 (d, J = 6.9 Hz, 2 H), 0.59 (d, J = 6.9 Hz, 1 H), 0.92 (d, J = 6.8 Hz, 2 H), 1.02 (d, J = 6.8 Hz, 1 H), 1.14 (d, J = 3.5 Hz, 3 H), 1.32 (s, 3 H), 1.82 (m, 1H), 3.57 (d, J= 8 Hz, 1H), 3.89 (s, 3H), 5.35 (s, 1H) 6.86 (dd, J = 6.3 and 2.3, 1H), 7.25 (dd, J= 8.0 and 1.15 Hz, 2H) ppm. ^{13}C NMR (500 MHz, $CDCl_3$): δ 17.14, 17.74, 18.87, 19.08, 23.06, 32.04, 46.82, 56.37, 79.60, 83.47, 87.12, 90.70, 111.10, 121.51, 122.92, 127.06, 139.32, 154.82 ppm.

5-(2-chloro-3-methoxyphenyl)-4-isopropyl-3,3-dimethyl-2,3-dihydrofuran **(6)** A solution of compound **5** (500 mg, 1.7 mmol) was prepared in toluene (5 mL). *p*-Toluenesulfonic acid monohydrate (30 mg, 0.17 mmol) was added and the mixture was refluxed for 2 hours. After that, the reaction was poured into satd aq $NaHCO_3$ and extracted with EtOAc. The organic layer was washed with brine, dried over Na_2SO_4 and concentrated. The residue was purified by chromatography on silica gel (2% EtOAc/Hexane) to afford compound **6** (0.124 g, 0.44 mmol, 26 %). ^{1}H-NMR (500 MHz, $CDCl_3$): δ 0.98 (d, J = 7.4 Hz, 6H), 1.25 (s, 6H), 2.33 (m, 1H), 3.89 (s, 3H), 3.99 (s, 2H), 6.39 (dd, J = 8.0 and 3.4, 2H), 7.25 (t, 1H) ppm. ^{13}C NMR (500 MHz, $CDCl_3$): δ 23.23, 25.06, 26.31, 46.54, 56.38, 82.53, 112.18, 122.99, 124.05, 125.42, 126.88, 134.50, 146.25, 155.32 ppm. HRMS calculated for $C_{16}H_{22}ClO_2$ [M+H+] 281.1308, found 281.1297

2-chloro-3-(3-isopropyl-4,4-dimethyl-4,5-dihydrofuran-2-yl)phenol **(7)** Compound **6** (400 mg, 1.42 mmol) was dissolved in 10 mL of dry DMF under nitrogen atmosphere. EtSNa (144 mg, 1.7 mmol) and Cs_2CO_3 (554 mg, 1.7 mmol) were added to the solution. The reaction was heated to 90 °C and stirred for 12 hours. After that, the mixture was poured into satd aq NH_4Cl and extracted with EtOAc. The organic layer was washed with brine, dried over Na_2SO_4 and concentrated. The residue was purified by chromatography on silica gel (10% EtOAc/Hexane) to afford compound **7** (0.231 g, 0.87 mmol, 61 %). ^{1}H-NMR (500 MHz, $CDCl_3$): δ 0.99 (d, J = 6.8 Hz, 6H), 1.25 (s, 6H), 2.35 (m, 1H), 3.99 (s, 2H), 6.90 (dd, J = 7.4 and 1.7, 1H), 7.01 (dd, J = 8.0 and 1.7, 1H) 7.15 (t, 1H) ppm. ^{13}C NMR (500 MHz, $CDCl_3$): δ 23.26, 25.02, 26.30, 46.52, 82.50, 116.31, 120.26, 123.92, 125.94, 127.55, 133.40, 145.91, 151.69 ppm. HRMS calculated for $C_{15}H_{20}ClO_2$ [M+H+] 267.1146, found 267.1154

2-chloro-6-iodo-3-(3-isopropyl-4,4-dimethyl-4,5-dihydrofuran-2-yl)phenol (8) Compound **7** (200 mg, 0.75 mmol) was dissolved in dry toluene under nitrogen atmosphere at 0 °C. NIS (169 mg, 0.75 mmol) was added in one portion and the reaction was stirred for 1 hour. The mixture was washed with brine and a few crystals of sodium thiosulfate pentahydrate were added to quench any iodine. The reaction was extracted with EtOAc, dried over Na_2SO_4 and concentrated. The residue was purified by chromatography on silica gel (5% EtOAc/Hexane) to afford compound **8** (0.129 g, 0.33 mmol, 44 %). ^{1}H-NMR (500 MHz, $CDCl_3$): δ 0.99 (d, J = 7.45 Hz, 6 H), 1.24 (s, 6 H), 2.35 (m, 1 H), 3.98 (s, 2 H), 6.67 (d, J = 8.0 , 1H), 7.61 (d, J = 8.0 and 1.7, 1H) ppm. ^{13}C NMR (500

MHz, $CDCl_3$): δ 23.27, 25.03, 26.27, 39.35, 46.54, 82.57, 119.75, 125.13, 126.45, 134.08, 136.88, 145.28, 151.22 ppm. HRMS calculated for $C_{15}H_{19}ClIO_2$ [M+H+] 393.0112, found 393.0121.

(E)-3-(3-chloro-2-hydroxy-4-(3-isopropyl-4,4-dimethyl-4,5-dihydrofuran-2-yl)phenyl)acrylonitrile **(9)** Compound **8** (120 mg, 0.3 mmol) was dissolved in dry MeCN (5 mL) under nitrogen atmosphere in a 10 mL microwave flask. Acrylonitrile (60 µL, 0.92 mmol), Et_3N (63 µL, 0.45 mmol) and $Pd(OAc)_2$ (0.015 mmol) were added to the solution. The reaction was microwaved at 120 °C for 70 minutes. The reaction was washed with satd aq NH_4Cl and brine. The organic layer was eluted with EtOAc, dried over Na_2SO_4 and concentrated. The residue was purified by chromatography on silica gel (10% EtOAc/Hexane) to afford compound **9** (0.0715 g, 0.225 mmol, 75 %). ^{1}H-NMR (500 MHz, $CDCl_3$): δ 1.00 (d, J = 6.85 Hz, 6 H), 1.25 (s, 6 H), 2.36 (m, 1 H), 3.99 (s, 2 H), 6.19 (d, J = 16.6, 1H), 6.95 (d, J = 8.05, 1H), 7.26 (d, J = 8.0, 1H), 7.54 (d, J = 16.6, 1H), ppm. ^{13}C NMR (500 MHz, $CDCl_3$): δ 23.17, 24.97, 26.16, 46.63, 82.57, 99.07, 118.41, 121.39, 121.67, 123.70, 126.79, 126.91, 135.57, 144.99, 145.16, 150.37 ppm. HRMS calculated for $C_{18}H_{21}ClNO_2$ [M+H+] 318.1255, found 318.1261

(E)-3-(3-chloro-2-hydroxy-4-(5-isopropyl-4,4-dimethyl-2,6,7-trioxabicyclo[3.2.0]heptan-1-yl)phenyl)acrylonitrile **(10)** A solution of compound **9** (70 mg, 0.22 mmol) and tetraphenylporphin (TPP) (1 mg) in DCM (5 mL) was irradiated externally with 120 W light bulb under an oxygen atmosphere at 0 °C. The reaction was monitored by TLC and the crude was purified by chromatography on silica gel (10% EtOAc/Hexane) to afford compound **10** (0.05 g, 0.143 mmol, 65 %). ^{1}H-NMR (500 MHz, $CDCl_3$): δ 0.85 (d, J = 6.3 Hz, 6H), 1.22 (s, 3H), 1.38 (s, 3H), 2.27 (m, 1H), 3.96 (d, J = 8.6 Hz, 1H), 4.53 (d, J = 7.45 Hz, 1H), 6.20 (d, J = 16.6 Hz, 1H), 6.40 (s, 1H), 7.33 (d, J = 2.25 Hz, 1H), 7.57 (d, J = 16.6 Hz, 1H) ppm. 13C NMR (500 MHz, $CDCl_3$): δ 16.49, 18.06, 19.24, 23.53, 29.23, 44.44, 80.46, 100.01, 104.35, 115.43, 118.17, 118.64, 121.16, 122.52, 126.99, 136.89, 144.72, 150.81 ppm. HRMS calculated for $C_{18}H_{21}ClNO_4$ [M+H+] 350.1153, found 350.1157

The monocyclic dioxetane was synthesized using the methodology previously reported[6] (Scheme **S2**)

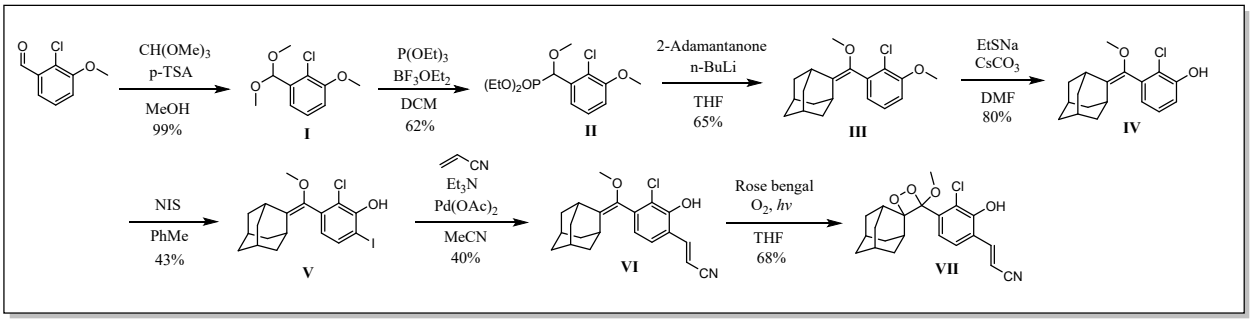

Scheme S2. Synthesis of monocyclic dioxetane **1**.

2-chloro-1-(dimethoxymethyl)-3-methoxybenzene (I). To a solution of 2-chloro-3-methoxybenzaldehyde(20 g, 112 mmol, 1.0 equiv) in 200 mL anhydrous methanol were added p-

Toluenesulfonic acid (1.5 mL, 11.2 mmol, 0.1 equiv) and trimethyl orthoformate (12.25 mL, 112 mmol, 1.0 equiv). The reaction was stirred at room temperature for 24 hr and washed with satd $NaHCO_3$ and brine upon completion. The organic layer was eluted with EtOAc, dried over Na_2SO_4 and concentrated to afford compound **I** as a colorless oil without further purification (24 g, 111 mmol, 99 %). ^{1}H NMR (500 MHz, $CDCl_3$) δ 7.23 (m, 2H), 6.90 (d, J= 6.85 Hz, 1H), 5.63 (s, 1H), 3.88 (s, 3H), 3.36 (s, 6H).

Diethyl ((2-chloro-3-methoxyphenyl)(methoxy)methyl)phosphonate (II). To an ice-cooled solution of compound **I** (**15 g, 69.2 mmol, 1.0 equiv**) in 100 mL anhydrous DCM was added boron trifluoride diethyl etherate (8.5 mL, 69.2 mmol, 1.0 equiv) dropwise under N_2 atmosphere and the reaction was stirred for 15 min. Then, triethyl phosphite (12.2 mL, 71.3 mmol, 1.03 equiv) was also added dropwise and stirred for an additional 10 min. The reaction was refluxed for 2 hr at 45 ºC and monitored by TLC. Upon completion, the mixture was washed with brine and eluted with DCM, dried with Na_2SO_4, filtered, and concentrated under reduced pressure. The residue was purified by chromatography on silica gel (50% EtOAc/Hexane) to afford compound **II** (13.85 g, 42.9 mmol, 62 %). ^{1}H NMR (500 MHz, $CDCl_3$) δ 7.28 (m, 2H), 6.89 (d, J= 2.9, 1H), 5.17 (d, *J* = 16.05 Hz, 1H), 4.17–4.21 (m, 4H), 3.89 (s, 3H), 3.32 (s, 1H), 1.31–1.35 (t, 3H, *J* = 6.8 Hz), 1.20–1.24 (t, 3H, *J* = 6.8 Hz).

(1*r*,3*r*,5*R*,7*S*)-2-((2-chloro-3-methoxyphenyl)(methoxy)methylene)adamantane(III). Compound **II** (10 g, 31 mmol, 1.0 equiv) was dissolved in 120 mL anhydrous THF under N_2 atmosphere. 2.6 M n-BuLi (14.3 mL, 37.2 mmol, 1.2 equiv) was added dropwise at -78 °C over 10 min period and the mixture was stirred for 20 min. After that, a solution of 2-adamantanone (5.6 g, 37.2 mmol, 1.2 equiv) in 25 mL anhydrous THF was introduced dropwise and allowed to stir for 5 min. The– 78 ºC bath was removed and the mixture was stirred for an additional 2 hr. After this period, the reaction was refluxed at 90 ºC for 3 hr. Upon completion as indicated by TLC, the reaction was cooled to room temperature, quenched with sat. NH_4Cl and extracted with EtOAc. The organic layer was dried over Na_2SO_4, and concentrated under reduced pressure. The residue was purified by chromatography on silica gel (5% EtOAc/Hexane) to afford compound **III** (6.4 g, 20.15 mmol, 65 %). ^{1}H NMR (500 MHz, $CDCl_3$) δ 7.15 (t, 1H, *J* = 7.6 Hz), 6.89–6.94 (m, 2H), 3.95 (s, 3H), 3.36 (s, 3H), 3.30 (s, 1H), 1.34-2.20 (m, 12H).

3-(((1*r*,3*r*,5*R*,7*S*)-adamantan-2-ylidene)(methoxy)methyl)-2-chlorophenol (IV). To a solution of compound **III** (5 g, 15.7 mmol, 1.0 equiv) in 50 mL anhydrous DMF were added sodium ethanethiolate (1.6 g, 18.84 mmol, 1.2 equiv) and Cs_2CO_3 (6.1 g, 18.84 mmol, 1.2 equiv) under N_2 atmosphere. The reaction was refluxed at 90 ºC and stirred for 12 hr. The mixture was washed with sat. NH_4Cl and brine, and eluted with 3 x 30 mL EtOAc. The organic layer was dried over Na2SO4, filtered, and concentrated under reduced pressure. The residue was purified by chromatography on silica gel (10 % EtOAc/Hexane) to afford compound **IV** (3.8 g, 12.56 mmol, 80 %). 1H NMR (500 MHz, $CDCl_3$) δ 7.15 (t, *J* = 7.5 Hz, 1H), 6.99 (d, *J* = 6.0 Hz, 1H), 6.83 (d, *J* = 6.0 Hz, 1H),5.69 (s, 1H), 3.30 (s, 3H), 3.29 (s, 1H), 1.70-2.01 (m, 13H).

3-(((1*r*,3*r*,5*R*,7*S*)-adamantan-2-ylidene)(methoxy)methyl)-2-chloro-6-iodophenol (V). To an ice-cooled solution of compound **IV** (3 g, 9.8 mmol, 1.0 equiv) in 50 mL anhydrous toluene was added *N*-Iodosuccinimide (2.2 g, 9.8 mmol, 1.0 equiv) under N_2 atmosphere. The reaction was stirred

for 1 hr at 0 ºC. Upon completion, as indicated by TLC, the reaction was washed with brine. Iodine was quenched by adding a few crystals of sodium thiosulfate pentahydrate (solution was changed from pink to colorless). The organic layer was eluted with EtOAc, dried over Na_2SO_4, and concentrated under reduced pressure. The crude residue was washed with hexane to afford compound **V** (1.8 g, 4.2 mmol, 43 %) as a white solid. ^{1}H NMR (500 MHz, $CDCl_3$) δ 7.61 (d, *J* = 8.0 Hz, 1H), 6.62 (d, *J* = 8.0 Hz, 1H), 6.12 (s, 1H), 3.30 (s, 3H), 3.28 (s, 1H), 1.63-2.11 (m, 13H).

(E)-3-(4-(((1r,3r,5R,7S)-adamantan-2-ylidene)(methoxy)methyl)-3-chloro-2 hydroxyphenyl)acrylonitrile **(VI).** In a 10 mL microwave flask, compound **V** (500 mg, 1.16 mmol, 1.0 equiv) was dissolved in 3 mL anhydrous MeCN under N_2 atmosphere. Acrylonitrile (0.22 mL, 3.48 mmol, 3.0 equiv), anhydrous Et_3N (0.24 mL, 1.74 mmol, 1.5 equiv), and $Pd(OAc)_2$ were added to the solution. The reaction was microwaved at 120 ºC for 70 min. Upon completion, as indicated by TLC, the reaction was washed with NH_4Cl and brine. The organic layer was eluted with EtOAc, dried over Na_2SO_4, filtered, and concentrated under reduced pressure. The residue was purified by chromatography on silica gel (10 % EtOAc/Hexane) to afford compound **VI** (165 mg, 0.464 mmol, 40 %) as a yellow solid. ^{1}H NMR (500 MHz, $CDCl_3$) δ 7.58 (d, *J* = 16.8 Hz, 1H), 7.27 (d, *J* = 8.0 Hz, 1H), 6.89 (d, *J* = 8.0 Hz, 1H), 6.30 (s, 1H), 6.18 (d, *J* = 16.8 Hz, 1H), 3.30 (s, 3H), 3.28 (s, 1H), 1.63-2.18 (m, 13H).

Monocyclic dioxetane (VII): Compound VI (100 mg, 0.281 mmol, 1 equiv) and a few milligrams of Rose Bengal were dissolved in 3 mL THF. The solution was irradiated externally with 120 W light bulb under an oxygen atmosphere at 0 °C. The reaction was monitored by TLC, the solvent was roto evaporated and the crude was purified by chromatography on silica gel (10 % EtOAc/Hexane) to afford monocyclic dioxetane (74 mg, 0.19 mmol, 68 %). ^{1}H NMR (500 MHz, $CDCl_3$) δ 1.17-2.16 (m, 13H), 3.01 (s, 1H), 3.21 (s, 3H), 6.23 (d, 1H, *J* = 17.12 Hz), 6.56 (s, 1H), 7.42 (d, 1H, *J* = 8.05 Hz), 7.60 (d, 1H, *J* = 17.12 Hz), 7.69 (d, 1H, *J* = 8.05 Hz) ppm. ^{13}C NMR (500 MHz, $CDCl_3$): δ 25.84, 26.17, 31.63, 32.20, 33.56, 34.14, 36.56, 49.78, 96.37, 100.15, 111.50, 118.26, 122.91, 124.97, 126.91, 134.89, 144.82, 150.76 ppm. HRMS calculated for $C_{21}H_{23}ClNO_4$ [M+H+] 388.1310, found 388.1319

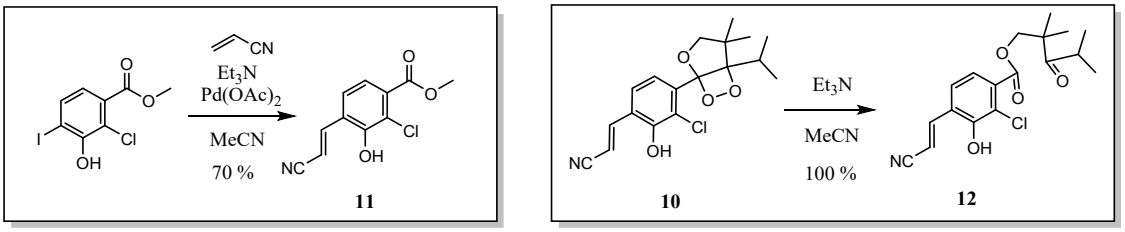

Scheme S3. Synthesis of the authentic emitter species.

methyl (E)-2-chloro-4-(2-cyanovinyl)-3-hydroxybenzoate **(11)** Methyl 2-chloro-3-hydroxy-4-iodobenzoate (30 mg, 0.096 mmol) was dissolved in dry MeCN (1 mL) under nitrogen atmosphere in a 10 mL microwave flask. Acrylonitrile (19 µL, 0.29 mmol), Et_3N (20 µL, 0.14 mmol) and

$Pd(OAc)_2$ (0.005 mmol) were added to the solution. The reaction was microwaved at 120 °C for 70 minutes. The reaction was washed with satd aq NH_4Cl and brine. The organic layer was eluted with EtOAc, dried over Na_2SO_4 and concentrated. The residue was purified by chromatography on silica gel (10 % EtOAc/Hexane) to afford compound **11** (16 mg, 0.0672 mmol, 70 %). ^{1}H NMR (500 MHz, $CDCl_3$): δ 3.94 (s, 3H), 6.25 (d, J = 16.6, 1H), 6.55 (s, 1H), 7.34 (d, J= 8.6, 1H), 7.49 (d, J= 8.6, 1H), 7.59 (d, J= 17.15, 1H) ppm. ^{13}C NMR (500 MHz, $CDCl_3$): δ 52.86, 100.81, 117.94, 120.82, 123.11, 124.39, 126.75, 131.30, 144.33, 150.77, 164.88 ppm. HRMS calculated for $C_{11}H_9ClNO_3$ [M+H+] 238.0265, found 238.0272

2,2,4-trimethyl-3-oxopentyl (E)-2-chloro-4-(2-cyanovinyl)-3-hydroxybenzoate (12) To a solution of 20 mg (0.057 mmol) of bicyclic dioxetane (**10**) in acetonitrile (1 mL) was added 10 µL of triethylamine and the mixture was stirred for 30 min at room temperature. The reaction was washed with satd aq NH_4Cl and the organic layer was eluted with EtOAc, dried over Na_2SO_4 and concentrated to afford compound **12** (20 mg, 0.057 mmol, 100 %). ^{1}H NMR (500 MHz, $CDCl_3$): δ 1.06 (d, J= 6.85, 6H), 1.27 (s, 6 H), 3.12 (m, 1H), 4.39 (s, 2H), 6.24 (d, J= 16.6, 1H), 7.31 (d, J=8.6, 1H), 7.42 (d, J= 8.6, 1H), 7.58 (d, J= 16.6, 1H) ppm. ^{13}C NMR (500 MHz, $CDCl_3$): δ 20.07, 21.66, 34.46, 48.18, 71.16, 101.06, 117.94, 120.78, 123.1591, 124.63, 126.62, 130.82, 144.50, 150.90, 164.27, 216.91 ppm. HRMS calculated for C18H21ClNO4 [M+H+] 350.1153, found 350.1162

Derivations of Cage Escape Model

The singlet quantum yield is expressed as the product of the yield of radical pair formation (ϕ_{rp}) and the yield of electron back transfer to the singlet excited state (ϕ_{ebt}) as shown in equation S7. ϕ_{ebt} is expressed as the ratio of the rate of electron back transfer (k_{ebt}) to the singlet excited state to the sum of k_{ebt} and the rate of cage escape k_{ce} as expressed in equation S8. This model assumes that (1) k_{ebt} is independent of viscosity, and (2) electron back transfer to the singlet excited state dominates over other electron back transfer products. Consideration of electron back transfer to singlet ground states and triplet excited states are more fully considered in the manuscript in equations 12–13. According to the Eigen equation,[7] the viscosity dependence of cage escape is expressed by equations S9–S11. Assuming that these constants are independent of viscosity, we embody these terms in the constant C_{CE} to give the simplified expression in equation S12.

$$\Phi_s = \phi_{rp}\phi_{ebt} \qquad \text{(Eq S7)}$$

$$\phi_{ebt} = \frac{k_{ebt}}{k_{ebt} + k_{ce}} \qquad \text{(Eq S8)}$$

$$k_{ce} = \frac{2kT}{\pi r^3 \eta} \frac{\frac{\omega_r}{RT}}{1 - e^{(\frac{-\omega_r}{RT})}} \qquad \text{(Eq S9)}$$

$$\omega_r = Z_a Z_b \left(\frac{e^2}{\varepsilon r}\right)\left(1 + \beta r \mu^{1/2}\right)^{-1} \quad \text{(Eq S10)}$$

$$\beta = \left(\frac{8\pi N^2 e^2}{1000 \varepsilon RT}\right)^{1/2} \quad \text{(Eq S11)}$$

$$k_{ce} = \frac{C_{ce}}{\eta} \quad \text{(Eq S12)}$$

Substitution of the expression for k_{ce} (Eq S12) into equation S8 gives equation S13. Simplification of the terms gives equations S14–S15, and then the reciprocal relation equation S16 is obtained, which gives equation S17 upon simplification. Equation S7 can be expressed as $\phi_{ebt} = \Phi_s / \phi_{rp}$ and substitution into equation S17 to give equation S18. Dividing both sides by ϕ_{rp}, we arrive at equation S19. Expressing this in terms of parameters A and B analogous to the collisional model [8,9] shows that ϕ_{rp} = 1/B (Eqs S20–S22), this is equal to Φ_s at large η. The parameter A is expressed in equation S23 and substitution of $C_{Ce} = k_{ce} / \eta$ (from Eq S12) provides equation S24 that can be rearranged to give an expression for the relative rates of electron back transfer to cage escape (k_{ebt} / k_{ce}) in equations S25–S26.

$$\phi_{ebt} = \frac{k_{ebt}}{k_{ebt} + \frac{C_{ce}}{\eta}} \quad \text{(Eq S13)}$$

$$\phi_{ebt} = \frac{k_{ebt}}{\frac{k_{ebt}\eta + C_{ce}}{\eta}} \quad \text{(Eq S14)}$$

$$\phi_{ebt} = \frac{k_{ebt}\eta}{k_{ebt}\eta + C_{ce}} \quad \text{(Eq S15)}$$

$$\frac{1}{\phi_{ebt}} = \frac{k_{ebt}\eta + C_{ce}}{k_{ebt}\eta} \quad \text{(Eq S16)}$$

$$\frac{1}{\phi_{ebt}} = 1 + \frac{C_{ce}}{k_{ebt}\eta} \quad \text{(Eq S17)}$$

$$\frac{\phi_{rp}}{\Phi_s} = 1 + \frac{C_{ce}}{k_{ebt}\eta} \quad \text{(Eq S18)}$$

$$\frac{1}{\boldsymbol{\Phi_s}} = \frac{1}{\boldsymbol{\phi_{rp}}} + \frac{C_{ce}}{\boldsymbol{\phi_{rp}} k_{ebt} \boldsymbol{\eta}} \quad \textbf{(Eq S19)}$$

$$\frac{1}{\Phi_s} = B + \frac{A}{\eta} \quad \text{(Eq S20)}$$

$$B = \frac{1}{\phi_{rp}} \quad \text{(Eq S21)}$$

$$\phi_{rp} = \frac{1}{B} \quad \text{(Eq S22)}$$

$$A = \frac{C_{ce}}{\phi_{cf} k_{ebt}} \quad \text{(Eq S23)}$$

$$A = \frac{k_{ce}\ \eta}{\phi_{rp} k_{ebt}} \quad \text{(Eq S24)}$$

$$\frac{k_{ce}}{k_{ebt}} = \frac{A\phi_{rp}}{\eta} \quad \text{(Eq S25)}$$

$$\frac{k_{ebt}}{k_{ce}} = \frac{\eta}{A\phi_{rp}} \quad \text{(Eq S26)}$$

Derivation of Molecular Reorientation Models

A similar derivation as above can be applied for the molecular reorientation model, with the key difference being in assuming that the viscosity dependence of a process that is undergoing molecular reorientation (as opposed to purely translational cage escape) has a viscosity dependence of $\eta^{-\alpha}$, which has been empirically observed as well as mathematically derived [10]. Thus, the rate of molecular reorganization (k_{or}) is given in terms of viscosity (η) and a constant C_{or} as expressed in equation S27. In this model, the yield of electron back transfer is expressed in equation 28, with similar assumptions as were used in the cage escape model. Similar steps as the cage escape model derived above can be applied (Equations S29–35). Equation S37 gives the estimate for ϕ_{rp} and equation S41 gives the estimate for k_{ebt}/k_{or}. It should be noted that equation S35 requires multiparameter non-linear fit to obtain the values for A, B, and α. The are described in the next section.

$$k_{or} = \frac{C_{or}}{\eta^{\alpha}} \quad \text{(Eq S27)}$$

$$\phi_{ebt} = \frac{k_{ebt}}{k_{ebt} + k_{or}} \quad \text{(Eq S28)}$$

$$\phi_{ebt} = \frac{k_{ebt}}{k_{ebt} + \frac{C_{or}}{\eta^{\alpha}}}$$ (Eq S29)

$$\phi_{ebt} = \frac{k_{ebt}}{\frac{k_{ebt}\eta^{\alpha} + C_{or}}{\eta^{\alpha}}}$$ (Eq S30)

$$\phi_{ebt} = \frac{k_{ebt}\eta^{\alpha}}{k_{ebt}\eta^{\alpha} + C_{or}}$$ (Eq S31)

$$\frac{1}{\phi_{ebt}} = \frac{k_{ebt}\eta^{\alpha} + C_{or}}{k_{ebt}\eta^{\alpha}}$$ (Eq S32)

$$\frac{1}{\phi_{ebt}} = 1 + \frac{C_{or}}{k_{ebt}\eta^{\alpha}}$$ (Eq S33)

$$\frac{\phi_{rp}}{\Phi_s} = 1 + \frac{C_{or}}{k_{ebt}\eta^{\alpha}}$$ (Eq S34)

$$\frac{1}{\boldsymbol{\Phi_s}} = \frac{1}{\boldsymbol{\phi_{rp}}} + \frac{C_{or}}{\boldsymbol{\phi_{rp}}\, k_{ebt}\boldsymbol{\eta^{\alpha}}}$$ **(Eq S35)**

$$\frac{1}{\Phi_s} = B + \frac{A}{\eta^{\alpha}}$$ (Eq S36)

$$\phi_{rp} = \frac{1}{B}$$ (Eq S37)

$$A = \frac{C_{or}}{\phi_{rp} k_{ebt}} \quad \text{(Eq S38)}$$

$$A = \frac{k_{ce}\, \eta^{\alpha}}{\phi_{rp}\, k_{ebt}} \quad \text{(Eq S39)}$$

$$\frac{k_{ce}}{k_{ebt}} = \frac{A \phi_{rp}}{\eta^{\alpha}} \quad \text{(Eq S40)}$$

$$\frac{k_{ebt}}{k_{ce}} = \frac{\eta^{\alpha}}{A \phi_{rp}} \quad \text{(Eq S41)}$$

Non-Linear Fits to the Molecular Reorientation

Viscosity dependence data for dioxetanes **1**—**2**, as well as dioxetanone **6**, diphenoyl peroxide **7**, and the peroxyoxalate system **8** (Manuscript Figure 7) were fit to equation S36 to obtain the parameters A, B, and α using Mathematica 13.1.

```
In[2]:= model = B + A * x^(-a);

In[3]:= data = {{0.890557, 1.35319}, {1.5777, 1.14039}, {4.32213, 1.06079},
    {10.1602, 1.01185}, {1.10902, 1.25402}, {1.46832, 1.23411},
    {2.15422, 1.14779}, {0.890557, 1.38308}};

In[4]:= fit = FindFit[data, {model, {B > 0, a > 0}}, {B, A, a}, x]

Out[4]= {B → 0.999975, A → 0.314929, a → 1.18985}

In[5]:= modelf = Function[{t}, Evaluate[model /. fit]]

Out[5]= Function[{t}, 0.999975 + 0.314929 / x^1.18985]

In[6]:= Plot[{modelf[t], 0}, {x, 0, 15}, Epilog → Map[Point, data]]
```

Out[6]=

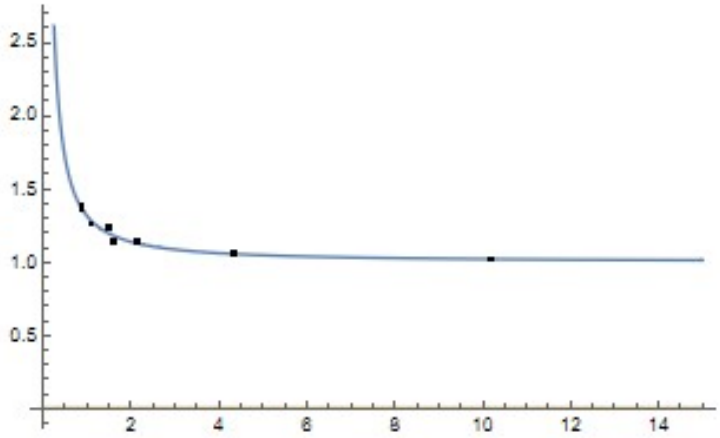


```
In[7]:= nlm = NonlinearModelFit[data, {model, {B > 0, a > 0}}, {B, A, a}, x]

Out[7]= FittedModel[ 0.999975 + 0.314929 / x^1.18985 ]

In[8]:= nlm[{"ParameterTable", "RSquared"}]
```

FittedModel: The property values {ParameterTable} assume an unconstrained model. The results for these properties may not be valid, particularly if the fitted parameters are near a constraint boundary.

Out[8]=

	Estimate	Standard Error	t-Statistic	P-Value
B	0.999975	0.0413203	24.2006	2.24524×10^{-6}
A	0.314929	0.0449724	7.00272	0.000915109
a	1.18985	0.332072	3.58311	0.0158227

, 0.999594

Figure S5. Mathematica notebook for non-linear fitting of the data for dioxetane **1** to the reorganization model described in equation S36.

```
In[1]:= model = B + A * x^ (-a);

In[2]:= data = {{0.890557, 2.16636}, {1.5777, 1.971}, {4.32213, 1.71209}, {10.1602, 1.66941},
    {1.10902, 2.10791}, {1.46832, 1.89115}, {2.15422, 1.77685}, {0.890557, 2.16896}};

In[3]:= fit = FindFit[data, {model, {B > 0, a > 0}}, {B, A, a}, x]

Out[3]= {B → 1.62495, A → 0.486801, a → 1.16376}

In[4]:= modelf = Function[{t}, Evaluate[model /. fit]]

Out[4]= Function[{t}, 1.62495 + 0.486801 / x^1.16376]

In[5]:= Plot[{modelf[t], 0}, {x, 0, 15}, Epilog → Map[Point, data]]
```

Out[5]=

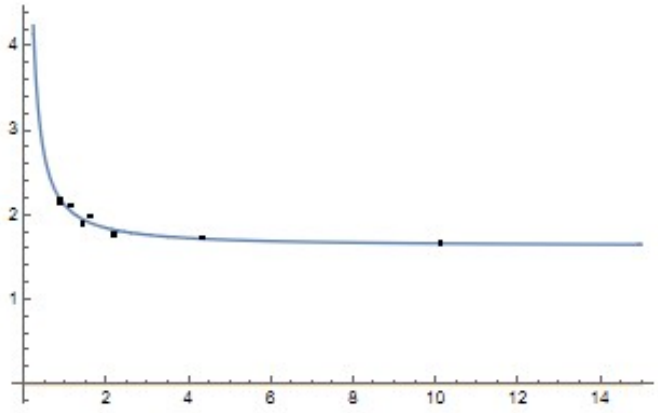


```
In[6]:= nlm = NonlinearModelFit[data, {model, {B > 0, a > 0}}, {B, A, a}, x]

Out[6]= FittedModel[1.62495 + 0.486801 / x^1.16376]

In[7]:= nlm[{"ParameterTable", "RSquared"}]

-- FittedModel: The property values {ParameterTable} assume an unconstrained model. The results for these properties may
   not be valid, particularly if the fitted parameters are near a constraint boundary.
```

Out[7]=

	Estimate	Standard Error	t-Statistic	P-Value
B	1.62495	0.0649469	25.0196	1.90324×10^{-6}
A	0.486801	0.0702874	6.92587	0.000962744
a	1.16376	0.328259	3.5453	0.0164696

, 0.999634

Figure S6. Mathematica notebook for non-linear fitting of the data for dioxetane **2** to the reorganization model described in equation S36.

```
In[1]:= model = B + A * x^ (-a);

In[2]:= data = {{0.56, 38167.9}, {0.82, 24937.7}, {1.05, 20408.2}, {1.37, 20000.}, {2.16, 18518.5},
    {2.57, 16129.}};

In[3]:= fit = FindFit[data, {model, {10 > a > 0, 10000 > B > 0, A > 0}}, {B, a, A}, x]

Out[3]= {B → 10000., a → 1.13579, A → 13705.}

In[4]:= modelf = Function[{t}, Evaluate[model /. fit]]

Out[4]= Function[{t}, 10000. + 13705. / x^1.13579]

In[6]:= Plot[{modelf[t], 0}, {x, 0, 15}, Epilog → Map[Point, data]]
```

Out[6]=

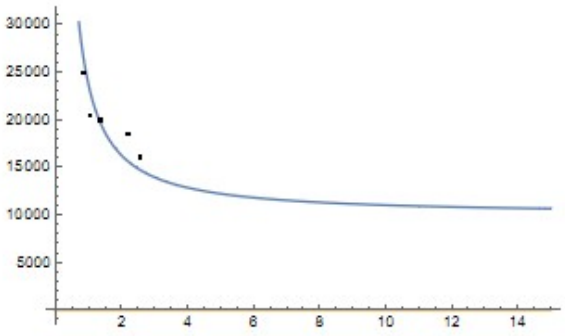


```
In[7]:= nlm = NonlinearModelFit[data,  {model, {10 > a > 0, 10000 > B > 0, A > 0}}, {B, a, A}, x]

Out[7]= FittedModel[ 10000. + 13705. / x^1.13579 ]

In[8]:= nlm[{"ParameterTable", "RSquared"}]

FittedModel: The property values {ParameterTable} assume an unconstrained model. The results for these properties may not be valid, particularly
if the fitted parameters are near a constraint boundary.
```

Out[8]=

	Estimate	Standard Error	t-Statistic	P-Value
B	10000.	8031.27	1.24513	0.30148
a	1.13579	0.729562	1.55681	0.217381
A	13705.	9325.23	1.46966	0.237993

, 0.993002

Figure S7. Mathematica notebook for non-linear fitting of the data for the activated dioxetanone system **6** to the reorganization model described in equation S36 using data tabulated in previous literature [11].

```
In[1]:= model = B + A * x^ (-a);

In[2]:= data = {{0.56, 4739.34}, {0.82, 4545.45}, {1.05, 4219.41}, {1.37, 3921.57},
          {2.16, 3690.04}, {2.57, 3355.7}};

In[3]:= fit = FindFit[data, {model, {10 > a > 0, A > 0, B > 3200}}, {B, A, a}, x]

Out[3]= {B → 3200., A → 967.588, a → 0.936793}

In[4]:= modelf = Function[{t}, Evaluate[model /. fit]]

Out[4]= Function[{t}, 3200. + 967.588 / x^0.936793]

In[5]:= Plot[{modelf[t], 0}, {x, 0, 15}, Epilog → Map[Point, data]]
```

Out[5]=

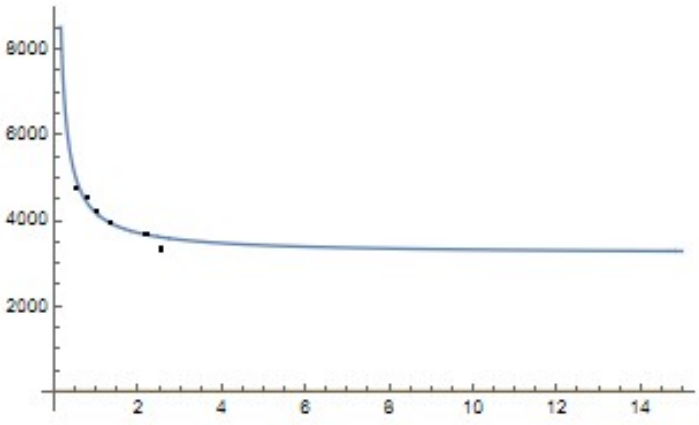


```
In[6]:= nlm = NonlinearModelFit[data, {model, {10 > a > 0, A > 0, B > 3200}}, {B, A, a}, x]

Out[6]= FittedModel[3200. + 967.588 / x^0.936793]

In[7]:= nlm[{"ParameterTable", "RSquared"}]

-- FittedModel: The property values {ParameterTable} assume an unconstrained model. The results for these
   properties may not be valid, particularly if the fitted parameters are near a constraint boundary.

Out[7]=
```

	Estimate	Standard Error	t-Statistic	P-Value
B	3200.	789.661	4.05237	0.0270695
A	967.588	880.844	1.09848	0.352251
a	0.936793	0.844063	1.10986	0.348021

, 0.99884

Figure S8. Mathematica notebook for non-linear fitting of the data for the activated diphenoyl peroxide system **7** to the reorganization model described in equation S36 using data tabulated in previous literature [11].

```
In[9]:= model = B + A * x^ (-a);

In[10]:= data = {{0.56, 454.545}, {0.7, 250.}, {0.82, 200.}, {1.05, 158.73}, {1.37, 91.7431}, {2.16, 50.2513}, {2.57, 50.}};

In[11]:= fit = FindFit[data, {model, {10 > a > 0}}, {B, A, a}, x]

Out[11]= {B → 45.303, A → 95.4491, a → 2.47088}

In[12]:= modelf = Function[{t}, Evaluate[model /. fit]]

Out[12]= Function[{t}, 45.303 + 95.4491 / x^2.47088]

         Plot[{modelf[t], 0}, {x, 0, 15}, Epilog → Map[Point, data]]
```

Out[ ]=

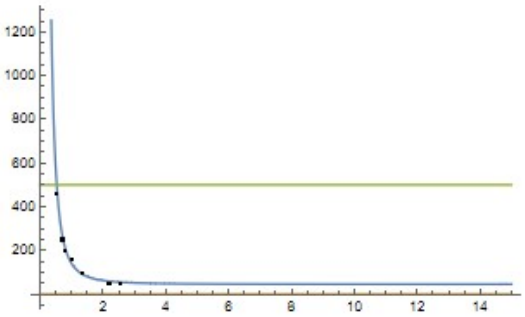


```
In[14]:= nlm = NonlinearModelFit[data, {model, {10 > a > 0}}, {B, A, a}, x]

Out[14]= FittedModel[45.303 + 95.4491 / x^2.47088]

In[15]:= nlm[{"ParameterTable", "RSquared"}]

         FittedModel: The property values {ParameterTable} assume an unconstrained model. The results for these properties may not be valid, particularly if the fitted
         parameters are near a constraint boundary.
```

Out[15]=

	Estimate	Standard Error	t-Statistic	P-Value
B	45.303	18.1802	2.49188	0.0673488
A	95.4491	22.7417	4.1971	0.0137278
a	2.47088	0.376698	6.5593	0.00279418

, 0.995128

Figure S9. Mathematica notebook for non-linear fitting of the data for the activated peroxyoxalate system **8** to the reorganization model described in equation S36 using data tabulated in in previous literature [9].

Computational Methods

The geometries of monocyclic dioxetane (Compound 1) and bicyclic dioxetane (Compound 2) were optimized using density functional theory (DFT) with the long-range separated ωB97XD functional [12] and the 6-311+G(d,p) basis set [13]. To investigate various conformations, potential energy surface (PES) was constructed through so-called relaxed scans calculations by systematically rotating the dihedral angle between the 1,2-dioxetane moiety and the benzene ring. For each geometry, the dihedral angle is fixed at the target angles from 0° to 350° in increments of 10°, i.e. 0°, 10°, 20°, …, 350°, while optimizing all other degrees of freedom of the molecule. For each optimized geometry with specific dihedral angle, the highest occupied

molecular orbital (HOMO) and lowest unoccupied molecular orbital (LUMO) energy gaps were calculated. All computations were carried out using the Gaussian 16 software package [14].

Scanned spectra

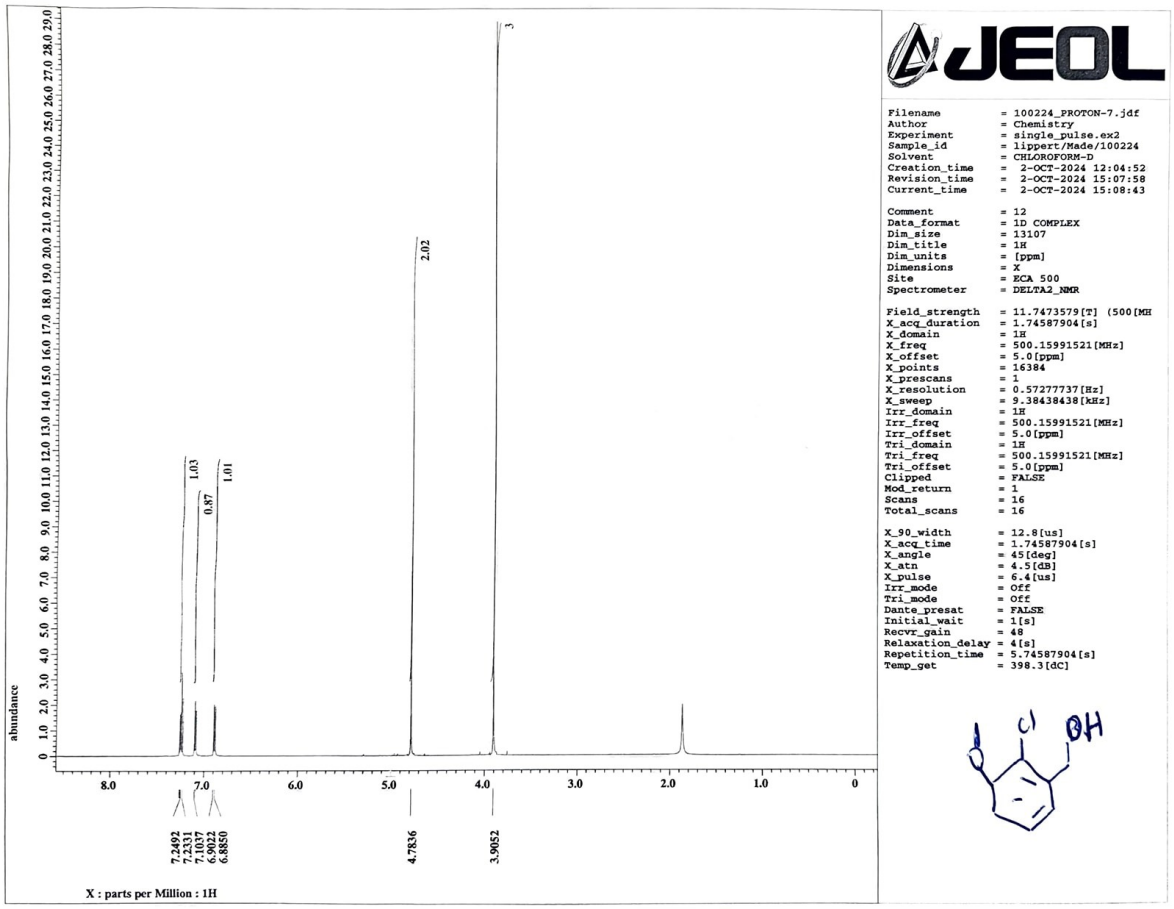

Figure S10. ^{1}H-NMR of compound **1** in $CDCl_3$

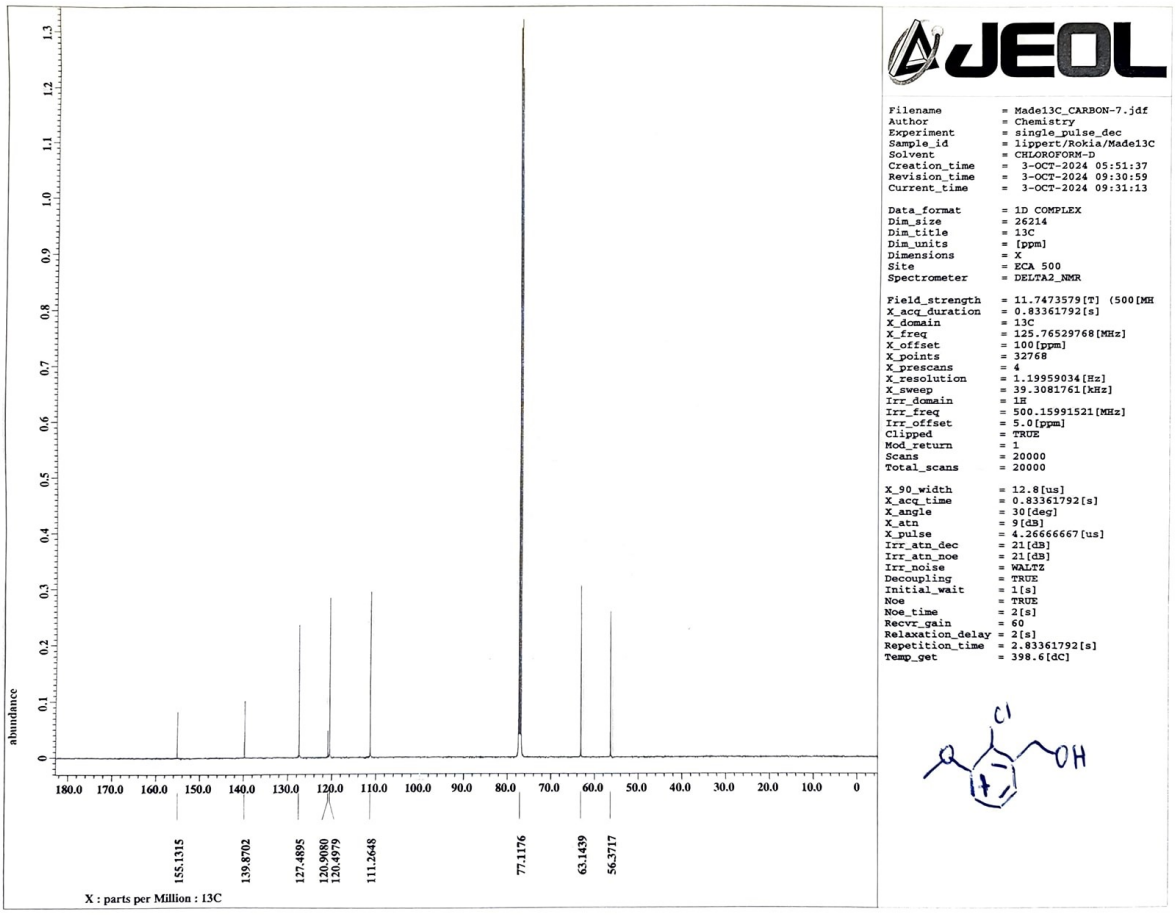

Figure S11. ^{13}C-NMR of compound **1** in $CDCl_3$.

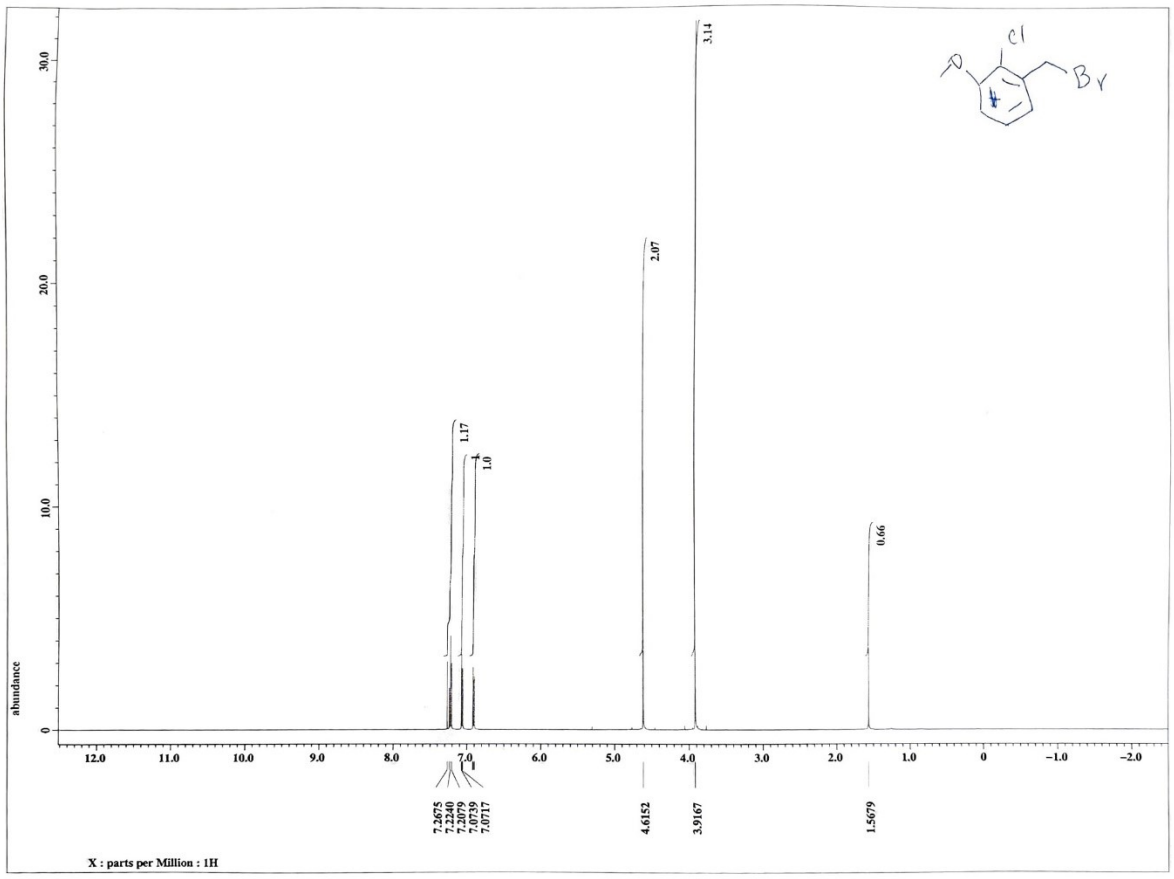

Figure S12. ^{1}H-NMR of compound **2** in $CDCl_3$

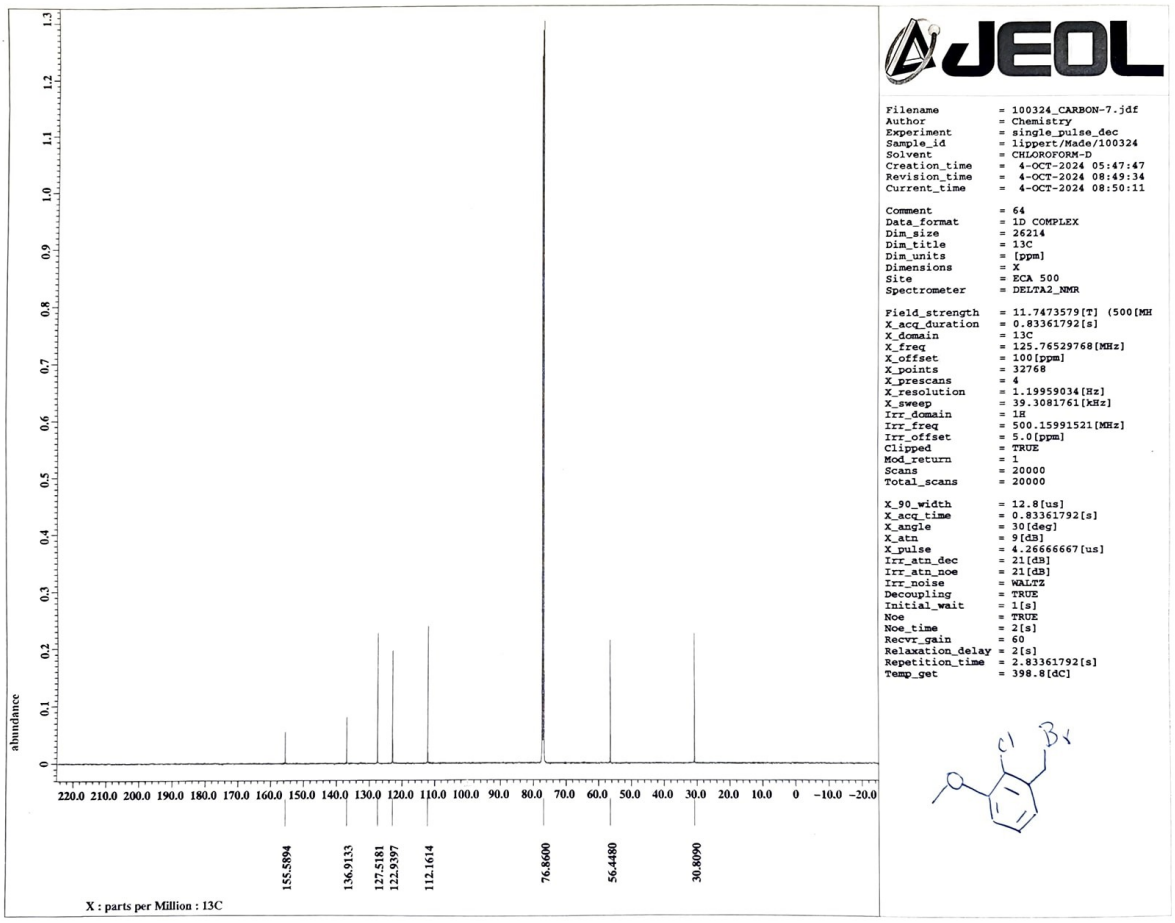

Figure S13. ^{13}C-NMR of compound **2** in $CDCl_3$.

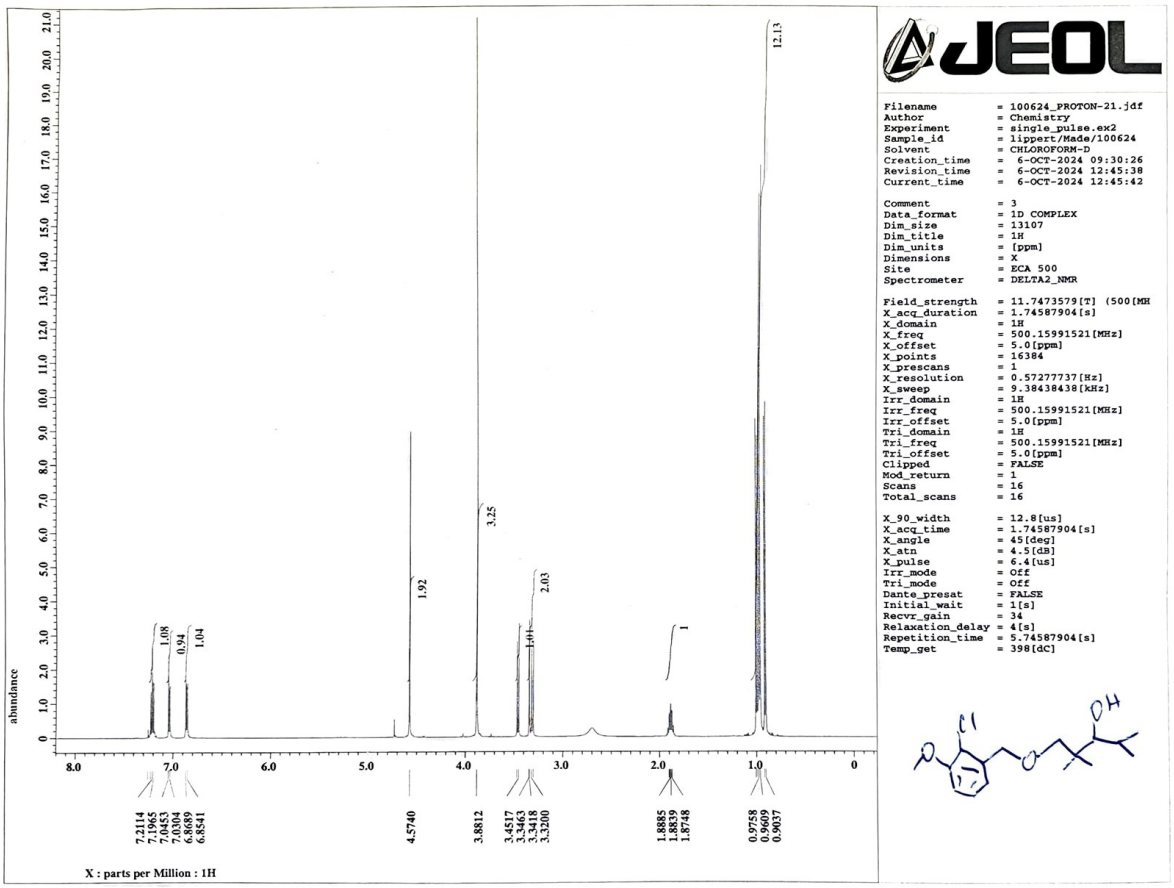

Figure S14: ^{1}H-NMR of compound **3** in $CDCl_3$

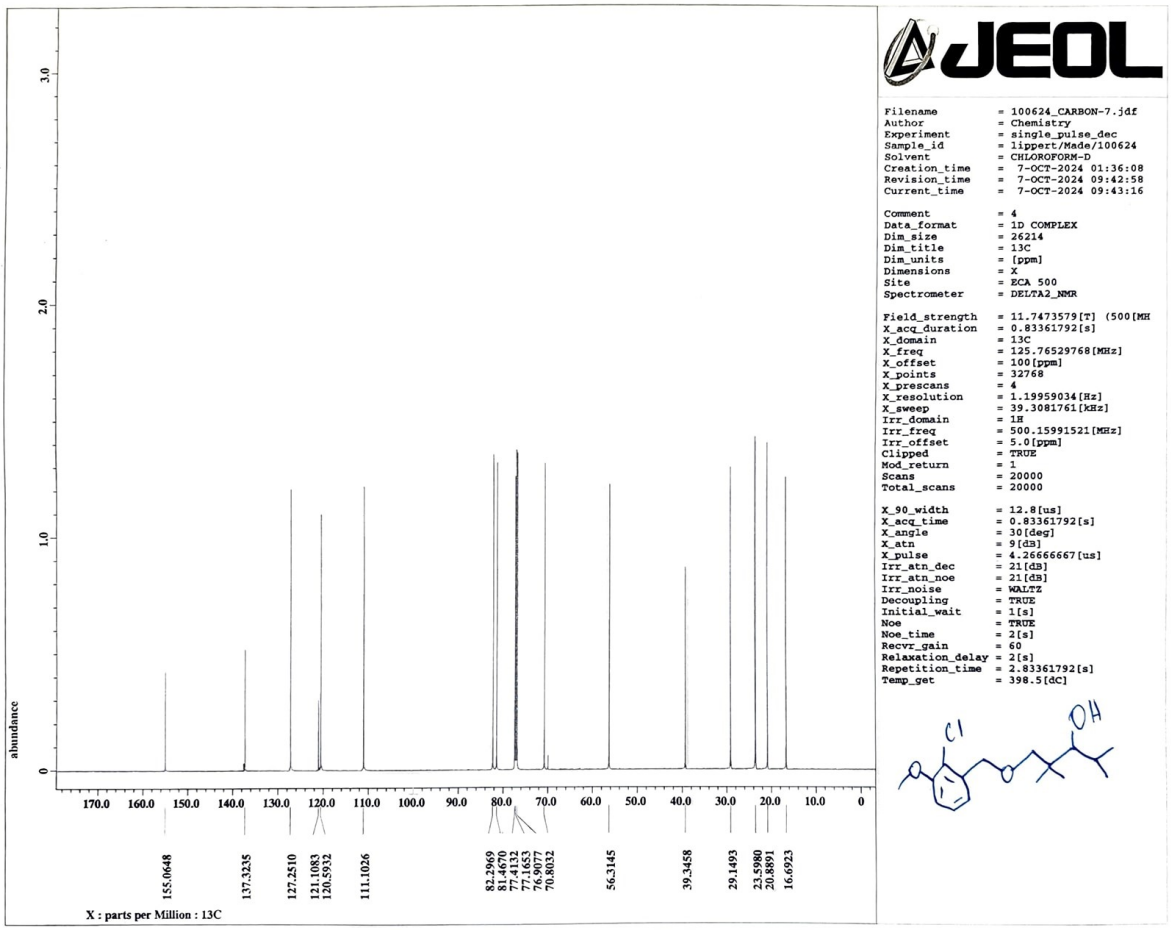

Figure S15: ^{13}C-NMR of compound **3** in $CDCl_3$.

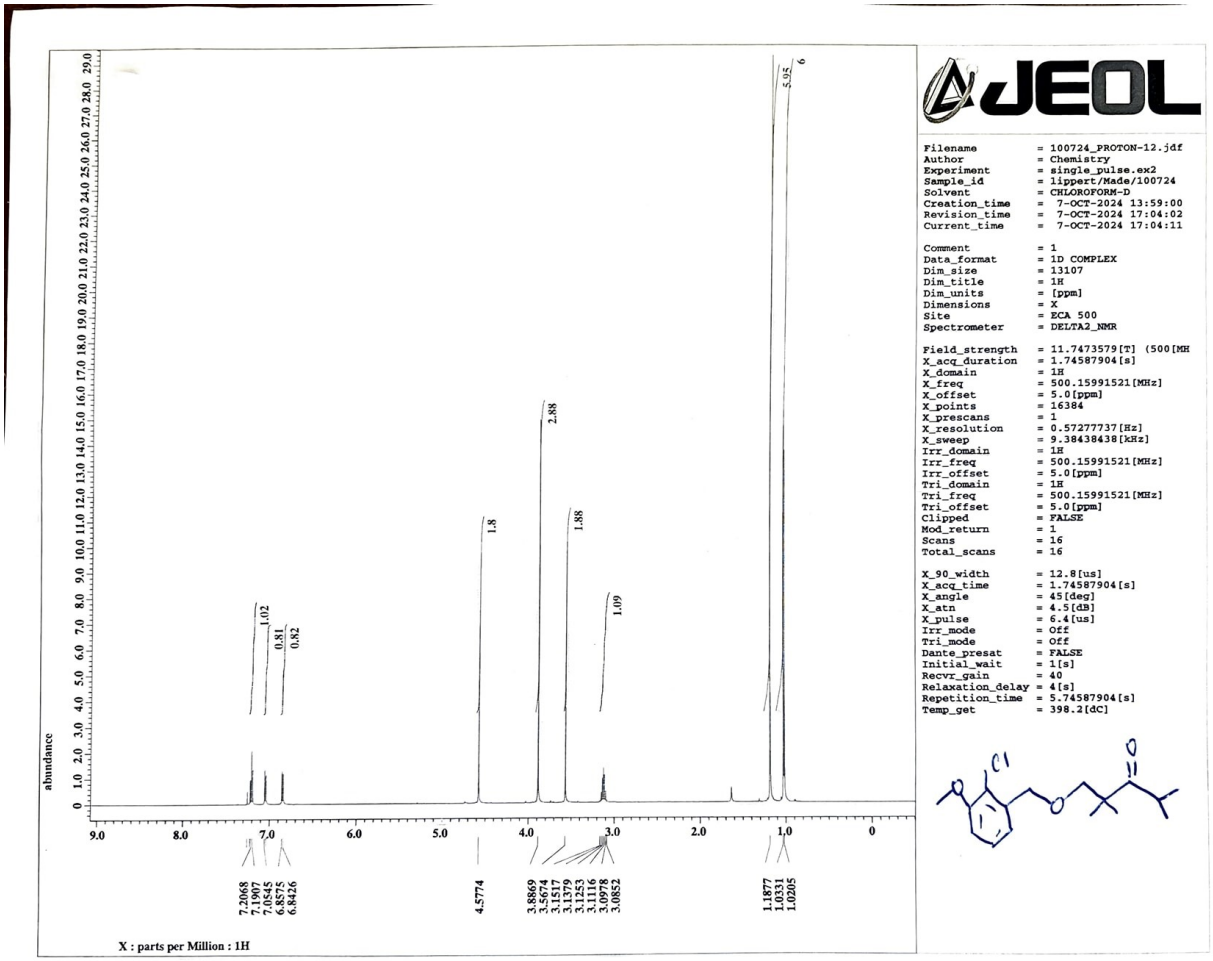

Figure S16: ^{1}H-NMR of compound **4** in $CDCl_3$

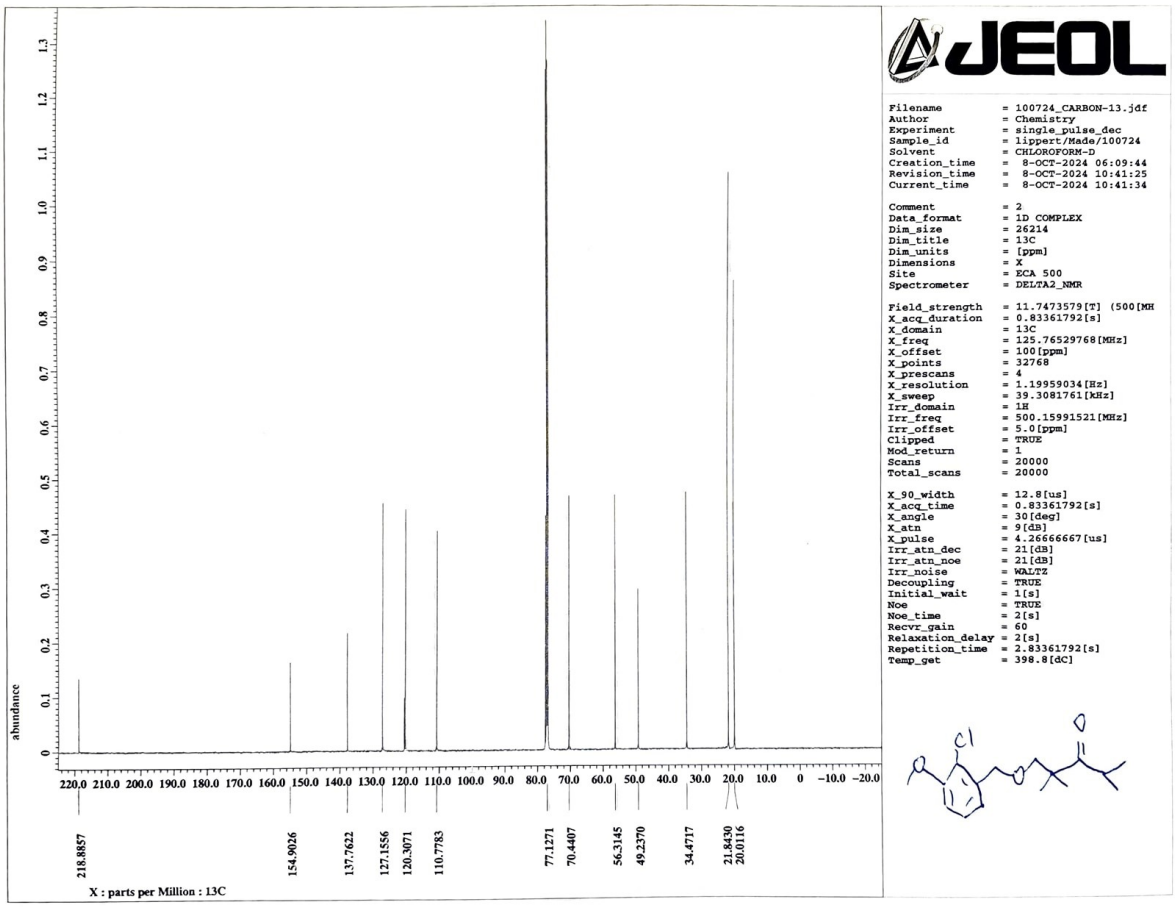

Figure S17: ^{13}C-NMR of compound **4** in $CDCl_3$.

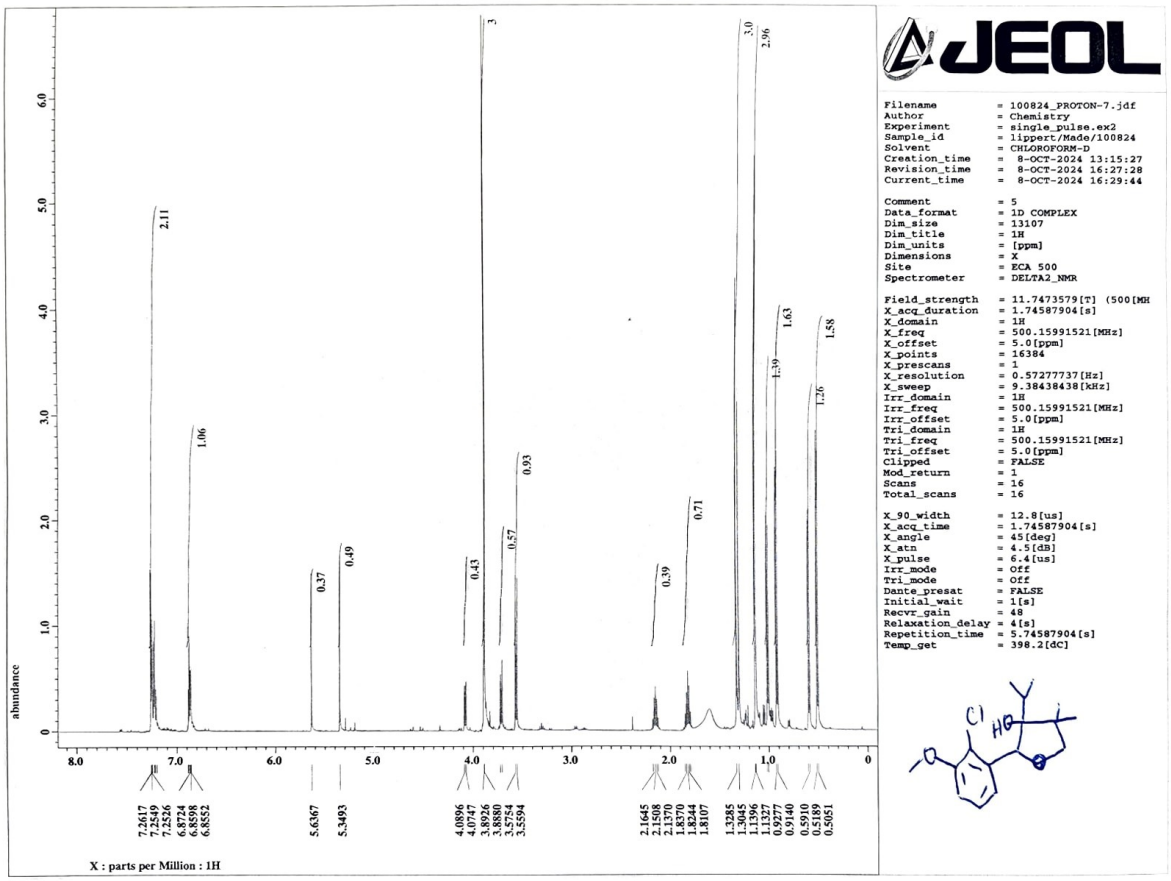

Figure S18: ^{1}H-NMR of compound **5** in $CDCl_3$

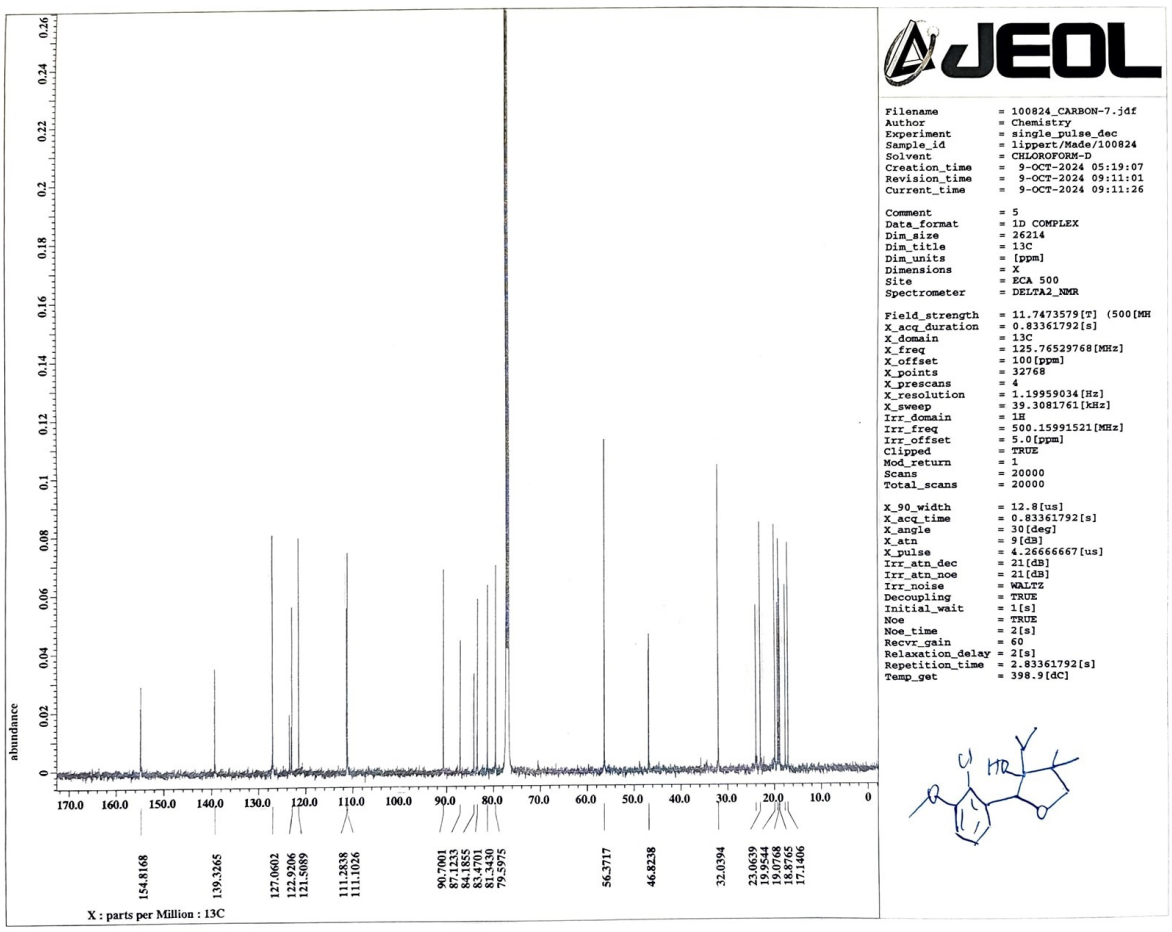

Figure S19: ^{13}C-NMR of compound **5** in $CDCl_3$.

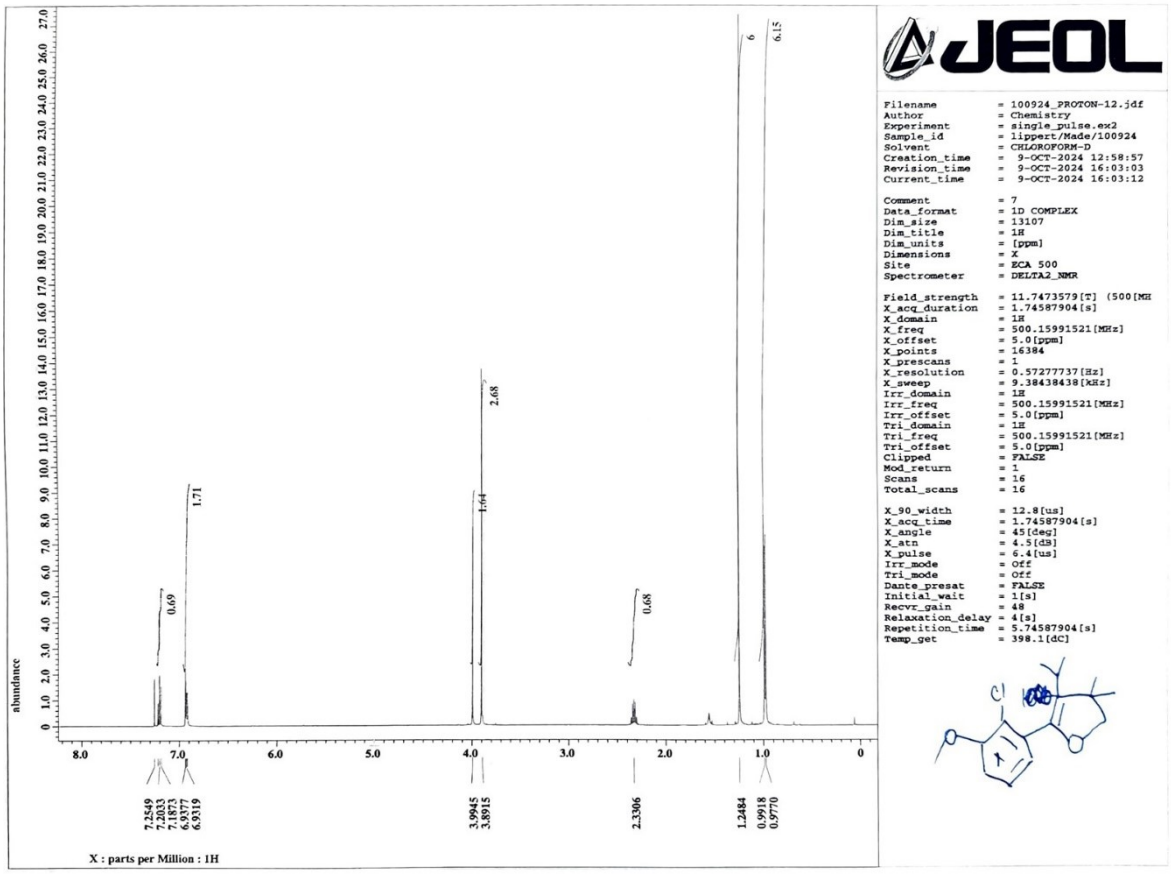

Figure S20: ^{1}H-NMR of compound **6** in $CDCl_3$

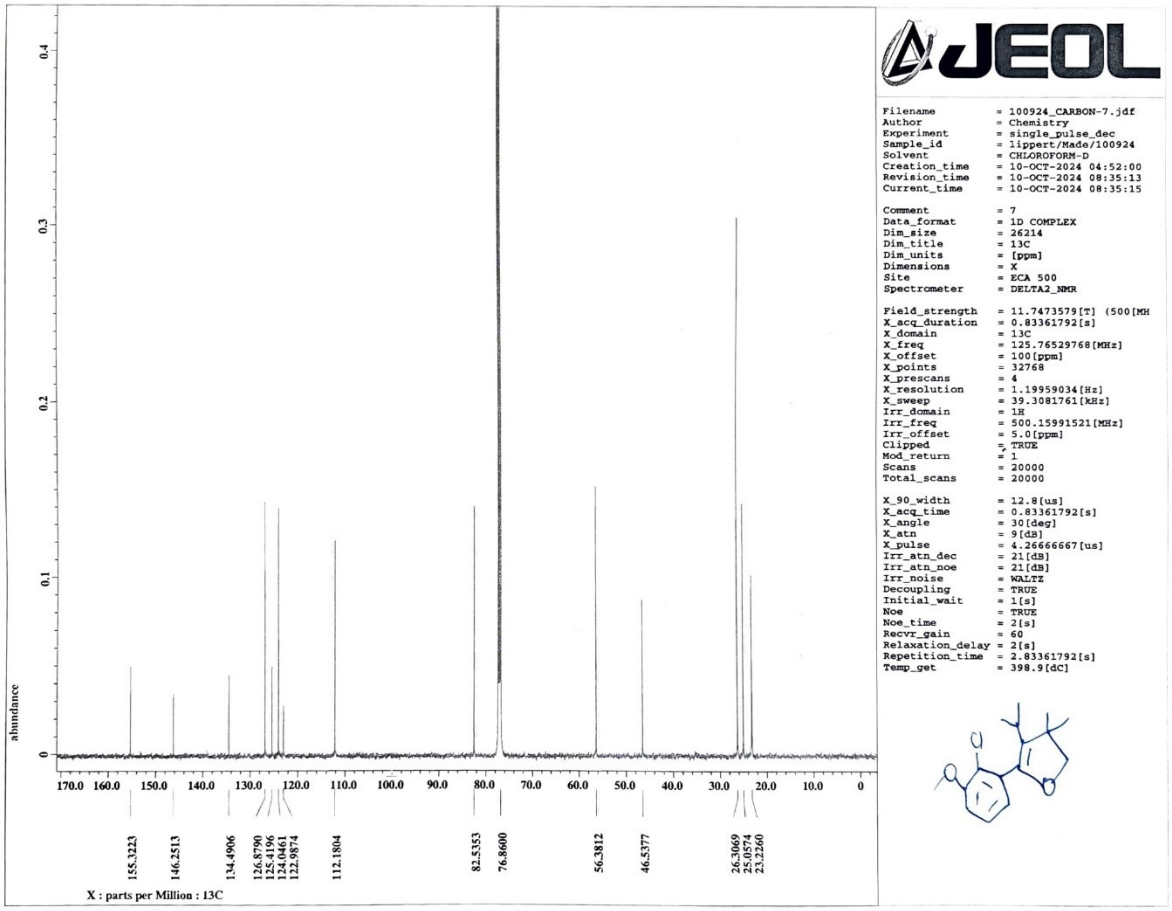

Figure S21: ^{13}C-NMR of compound **6** in $CDCl_3$.

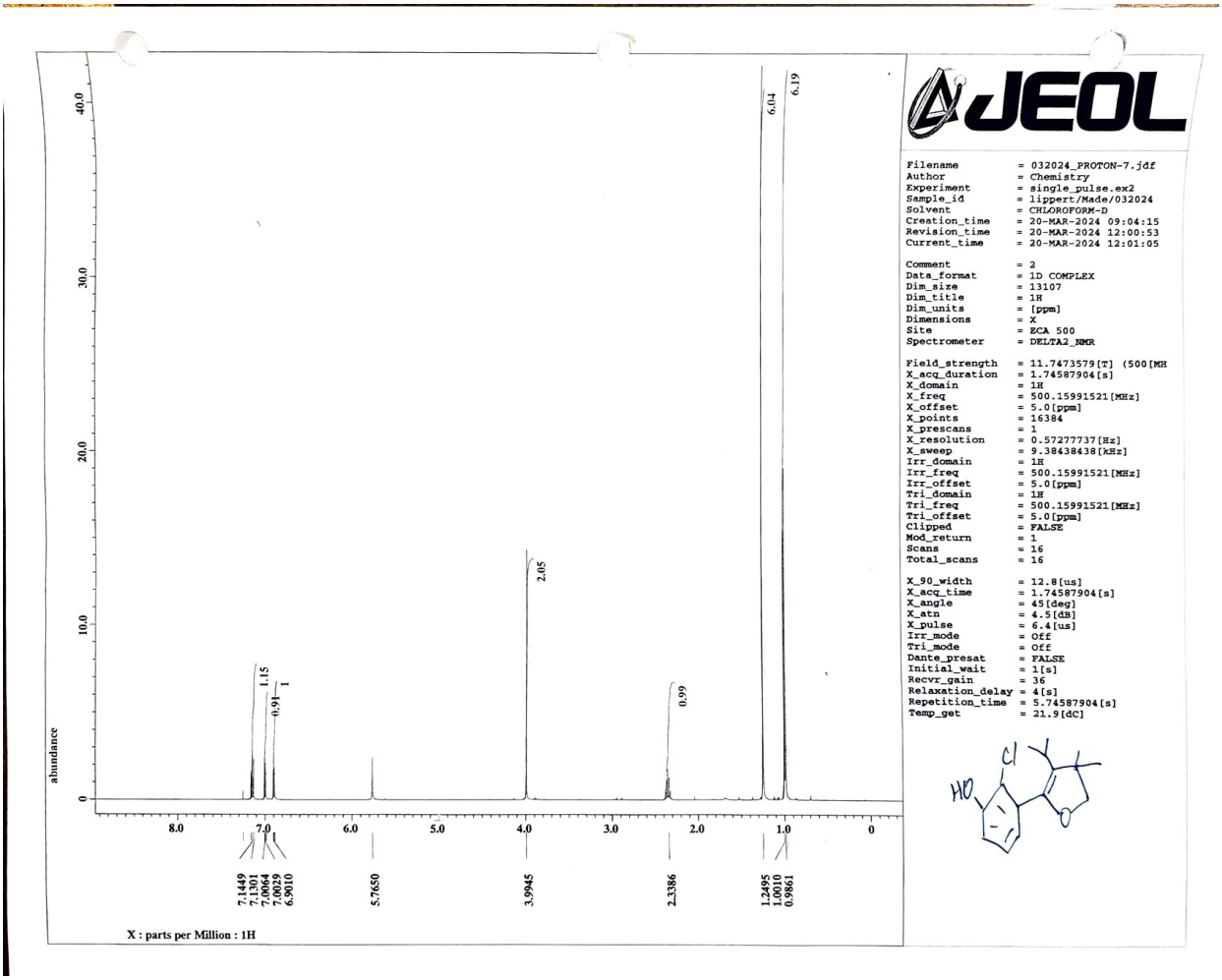

Figure S22: ^{1}H-NMR of compound **7** in $CDCl_3$

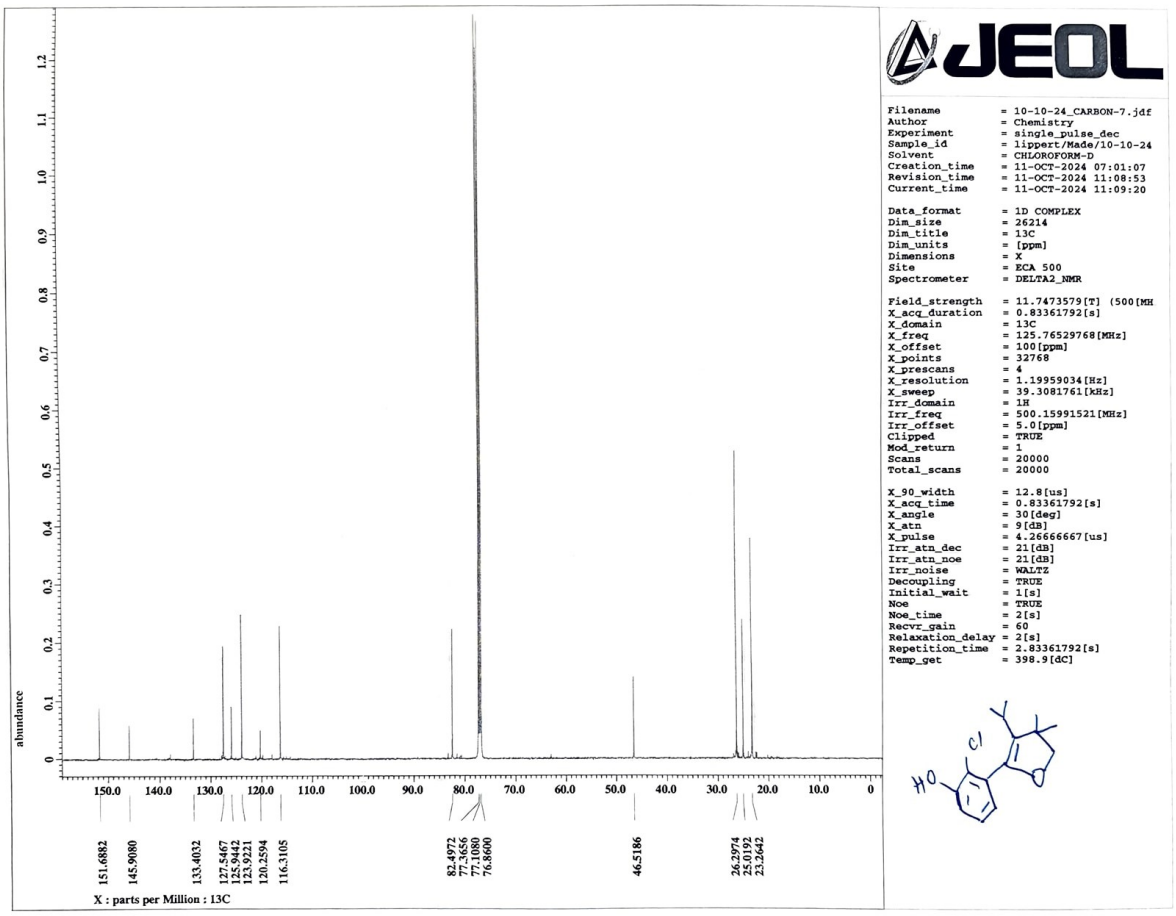

Figure S23: ^{13}C-NMR of compound **7** in $CDCl_3$.

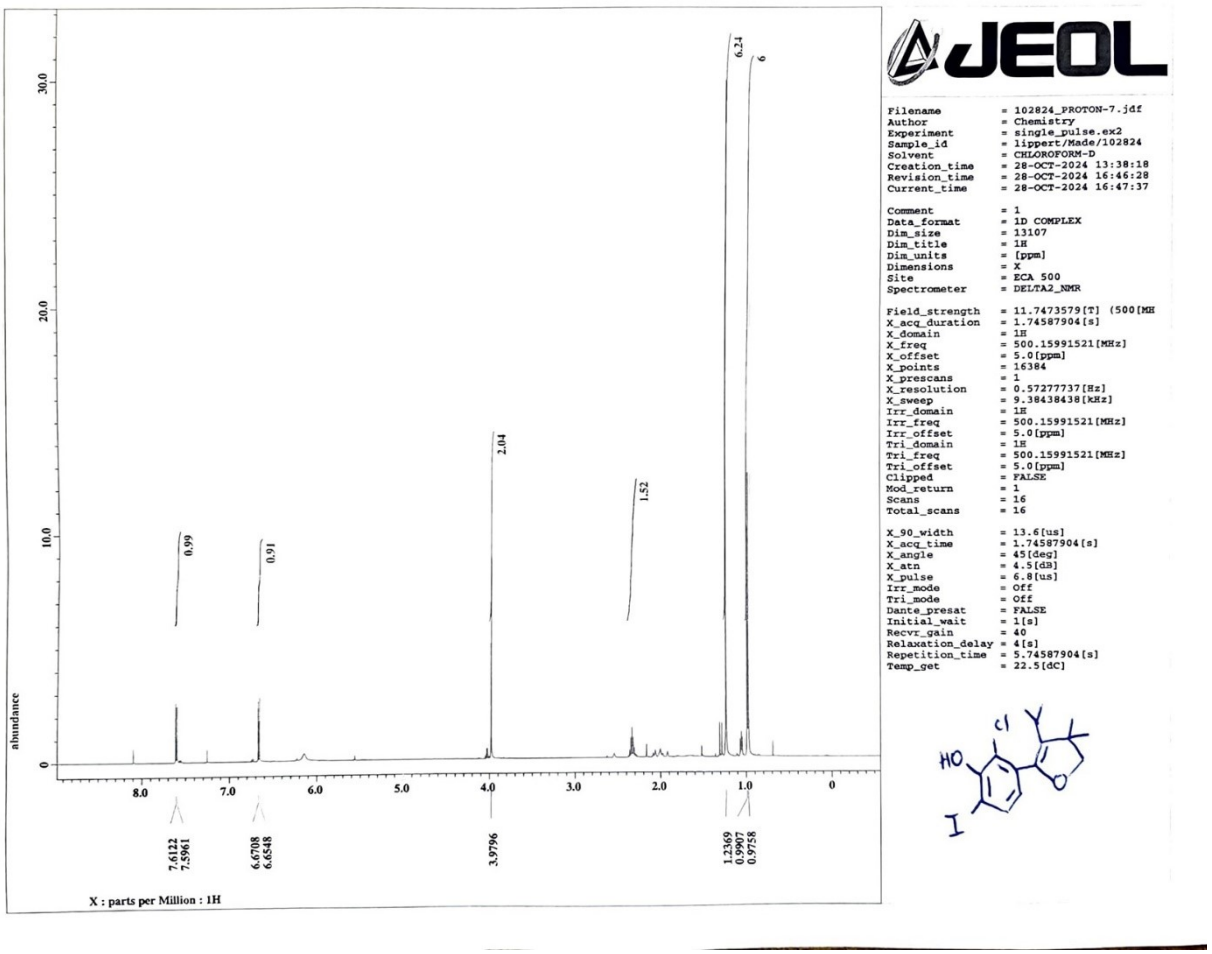

Figure S24: ^{1}H-NMR of compound **8** in $CDCl_3$

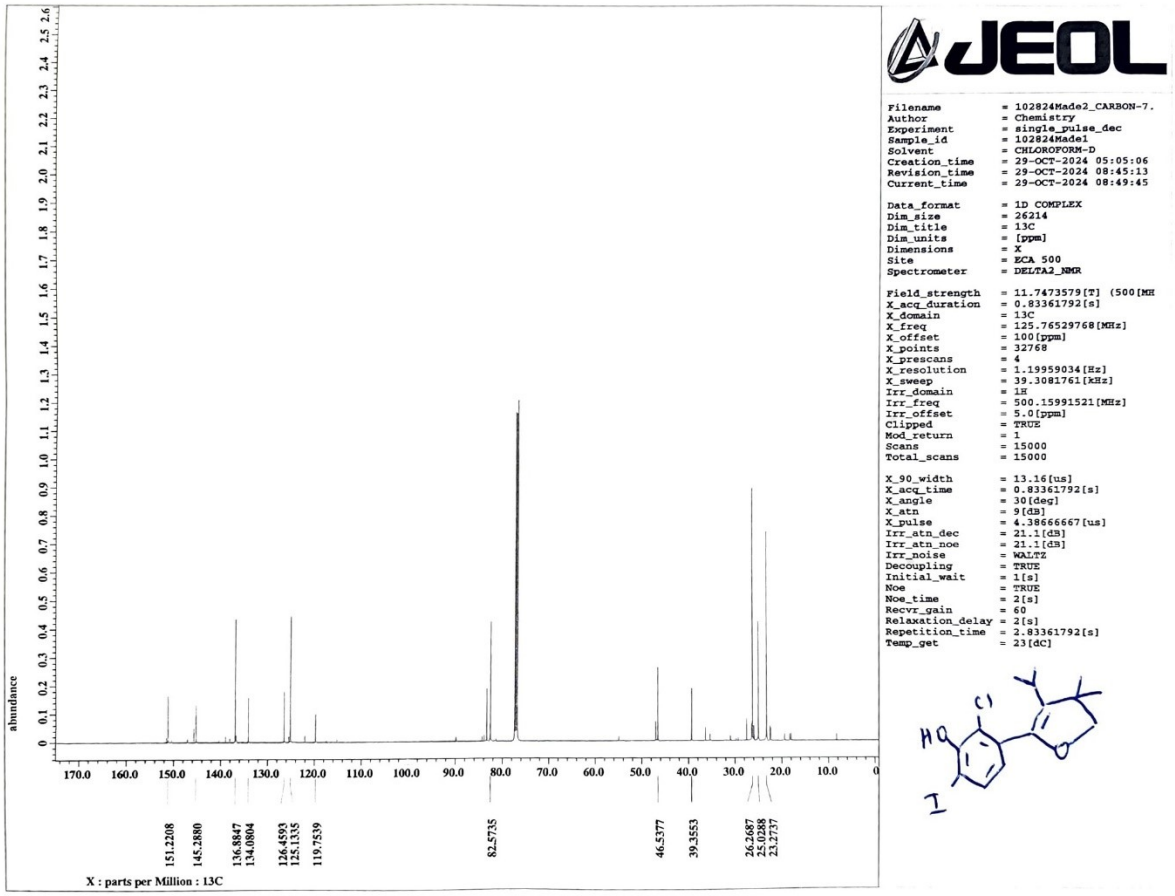

Figure S25: ^{13}C-NMR of compound **8** in $CDCl_3$.

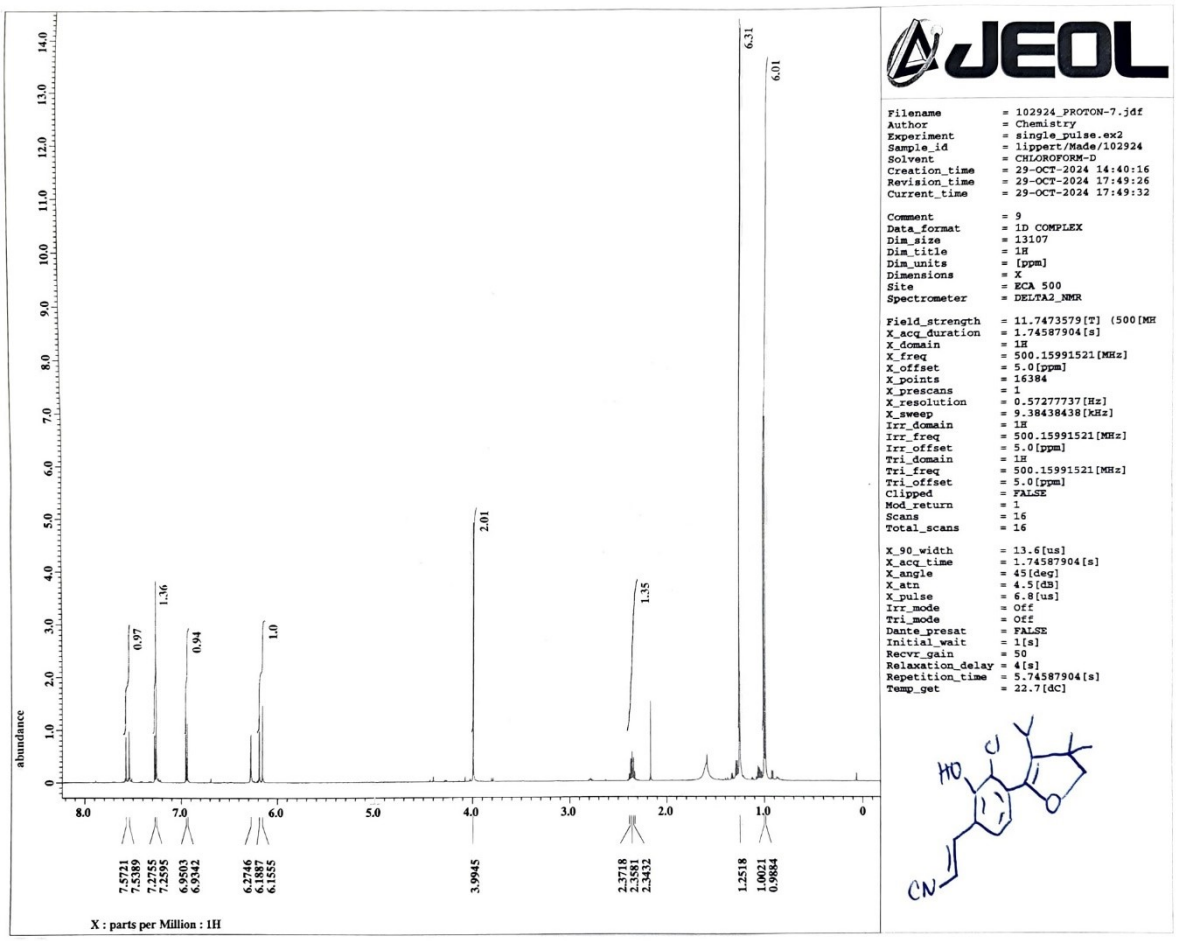

Figure S26: ^{1}H-NMR of compound **9** in $CDCl_3$

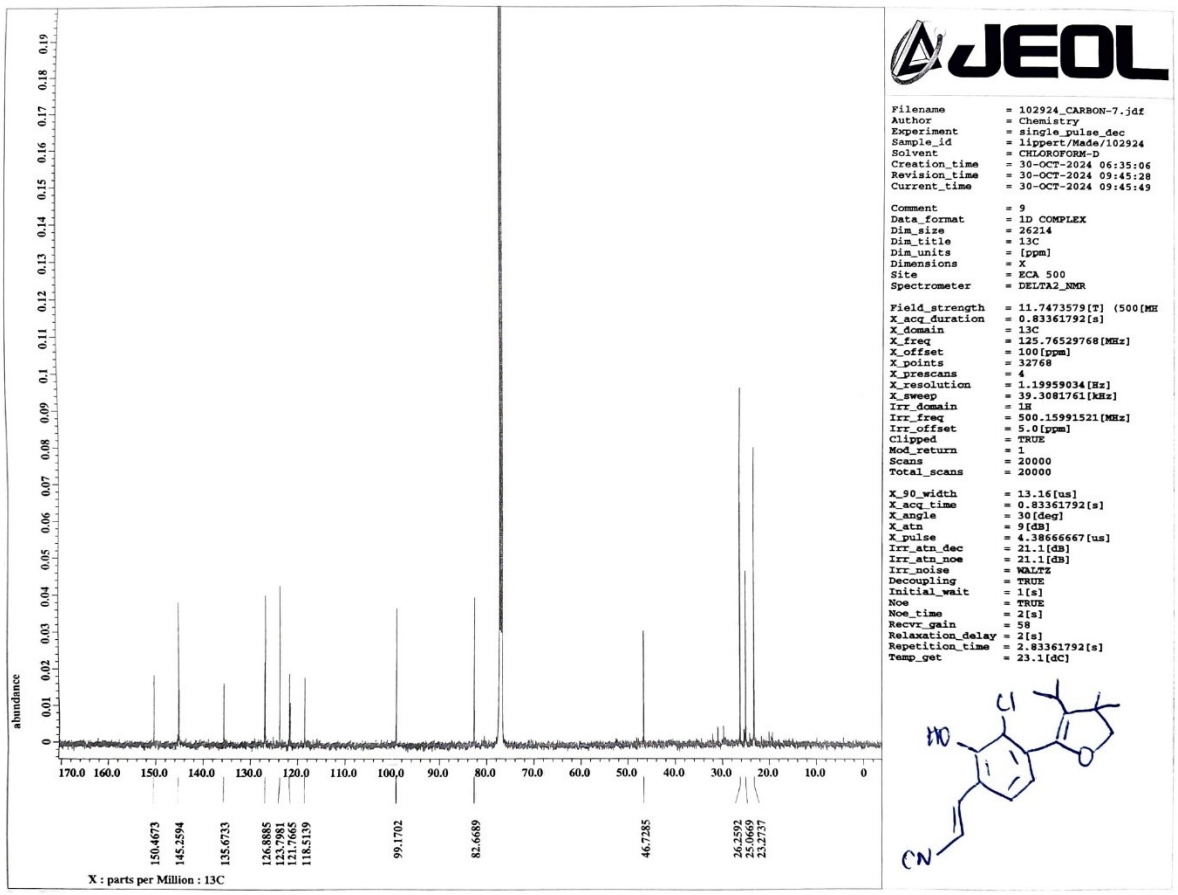

Figure S27: ^{13}C-NMR of compound **9** in $CDCl_3$.

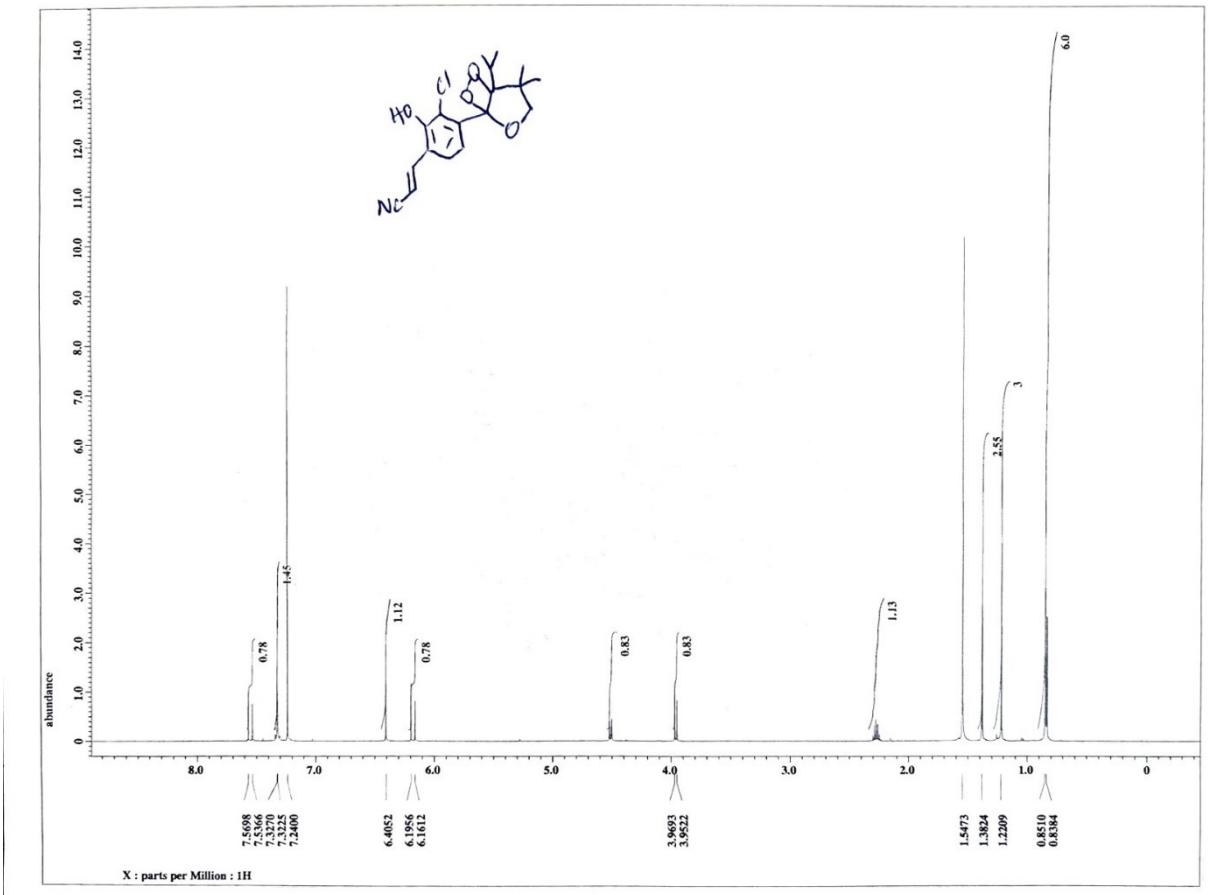

Figure S28: ^{1}H-NMR of compound **10** in $CDCl_3$

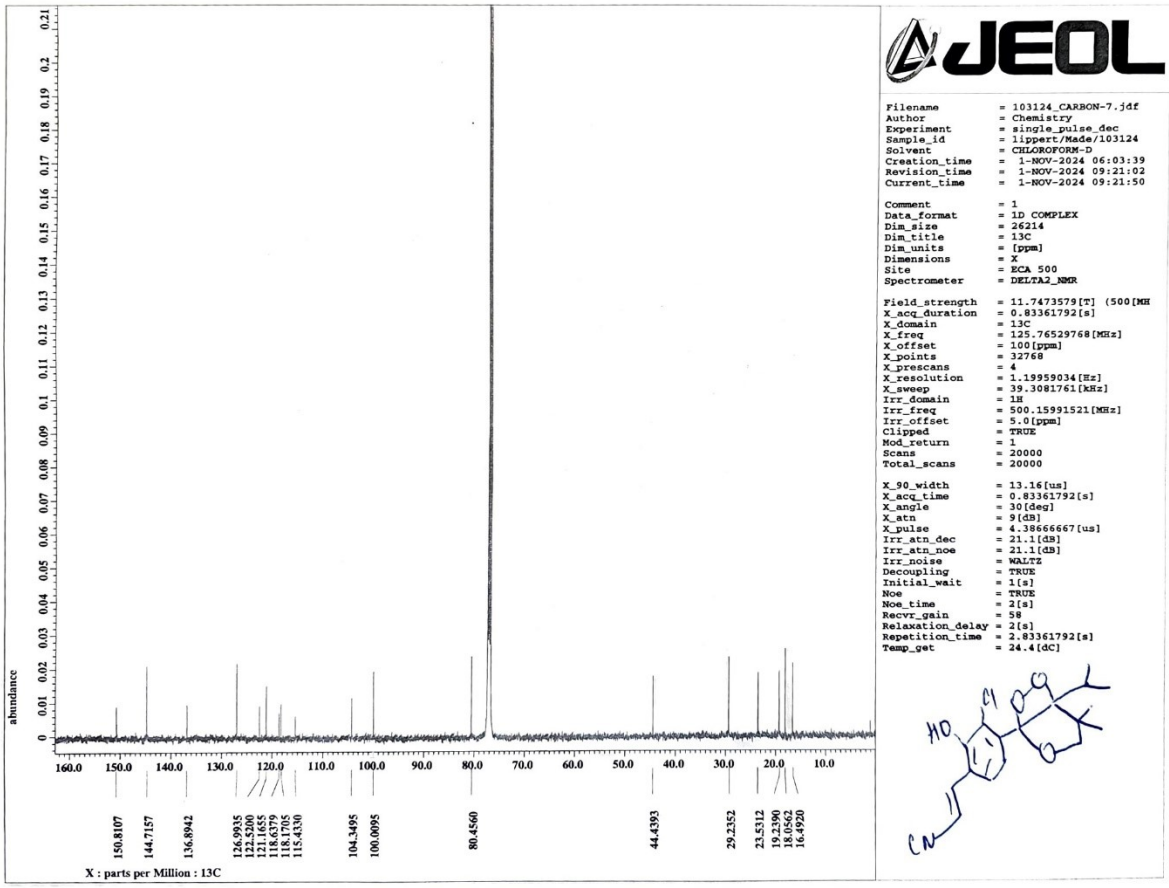

Figure S29: ^{13}C-NMR of compound **10** in $CDCl_3$.

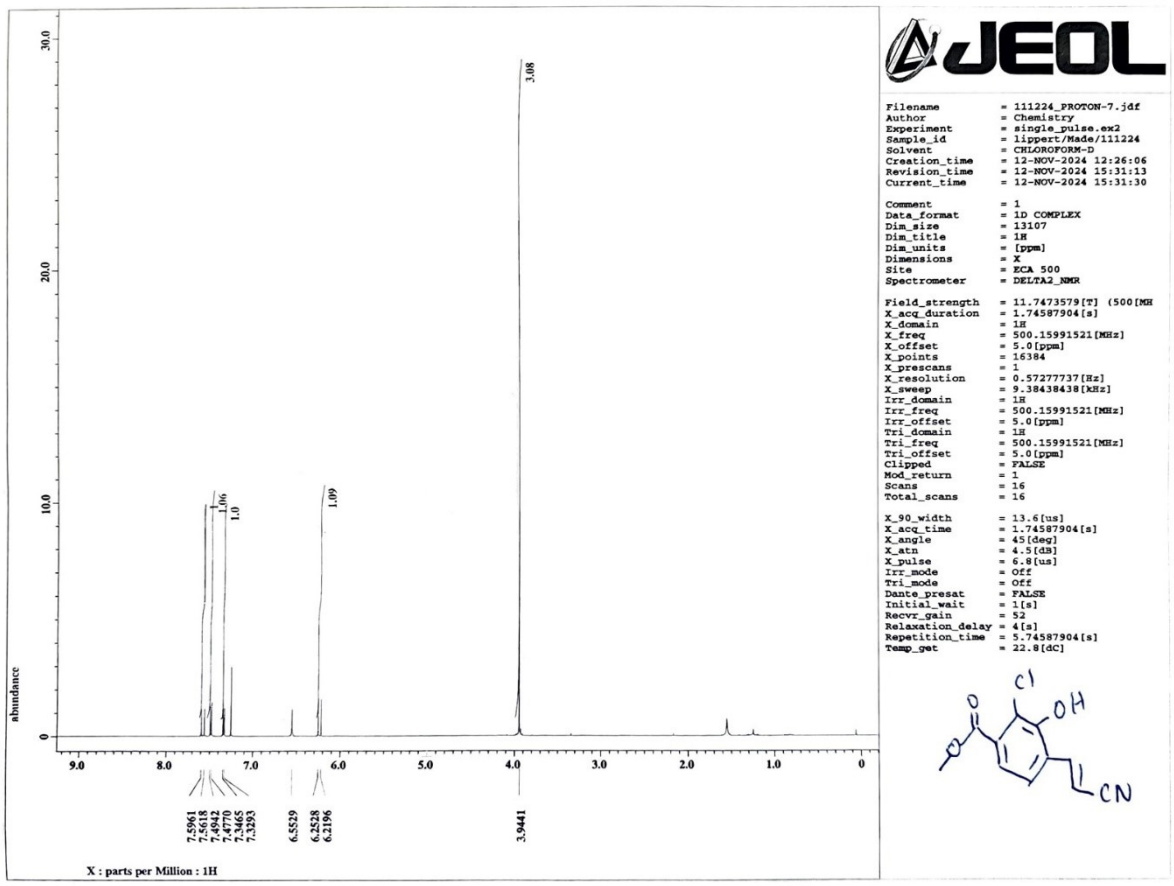

Figure S30: ^{1}H-NMR of compound **11** in $CDCl_3$

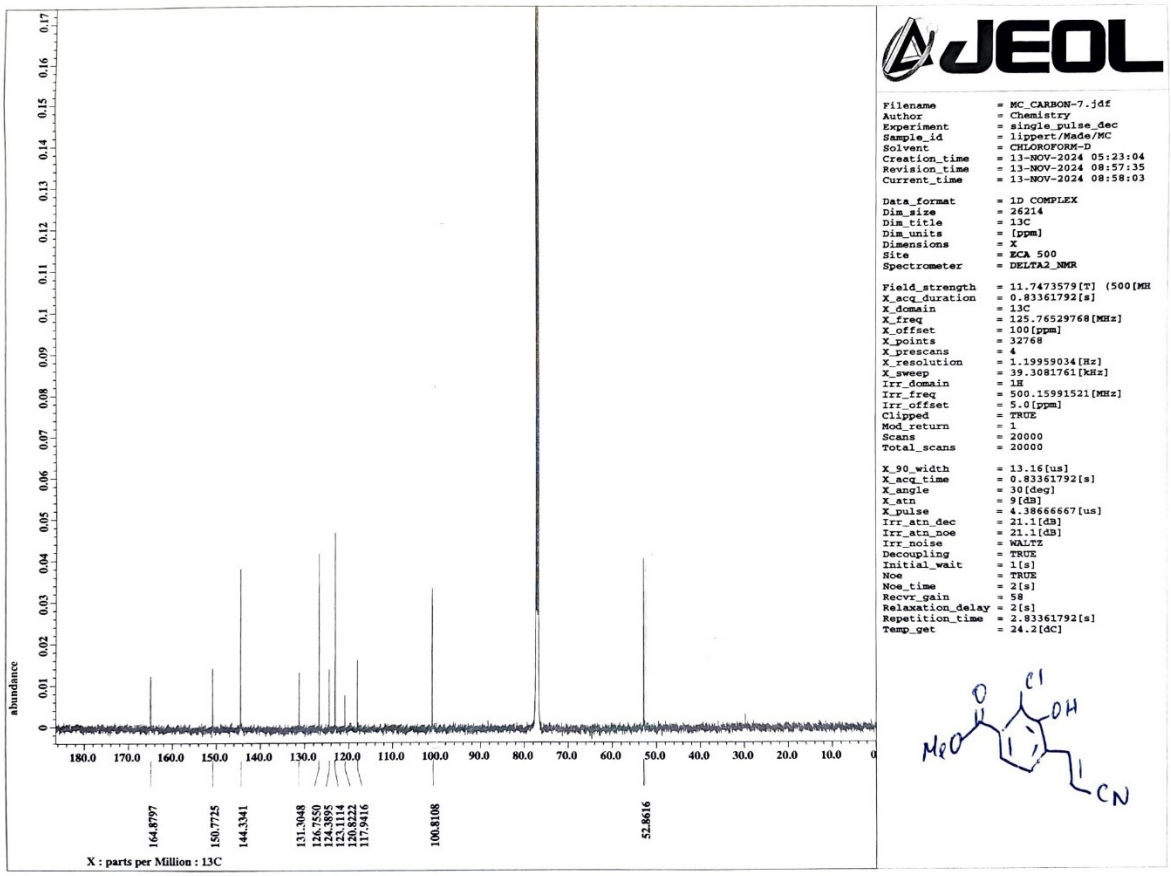

Figure S31: ^{13}C-NMR of compound **11** in $CDCl_3$.

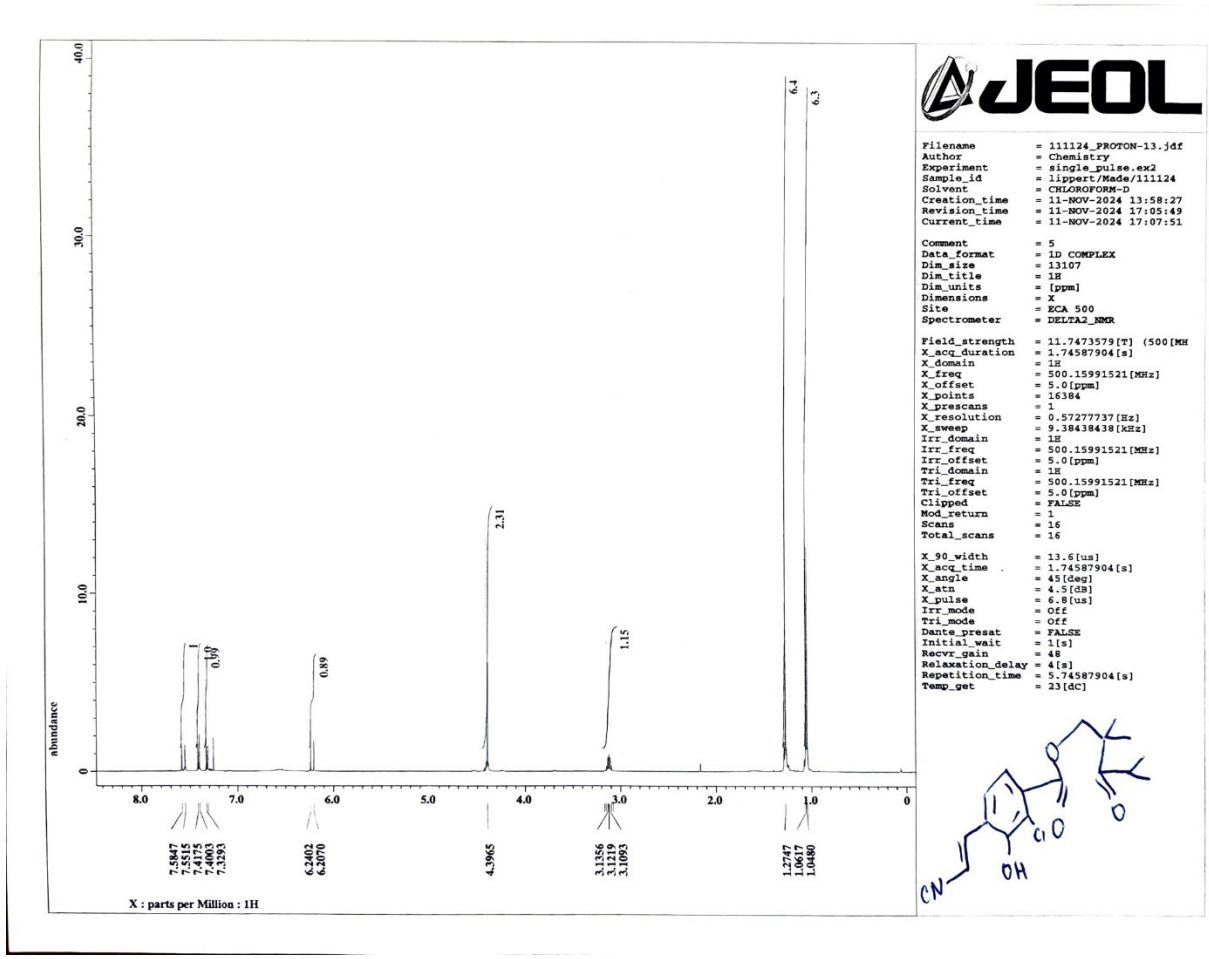

Figure S32: ^{1}H-NMR of compound **12** in $CDCl_3$

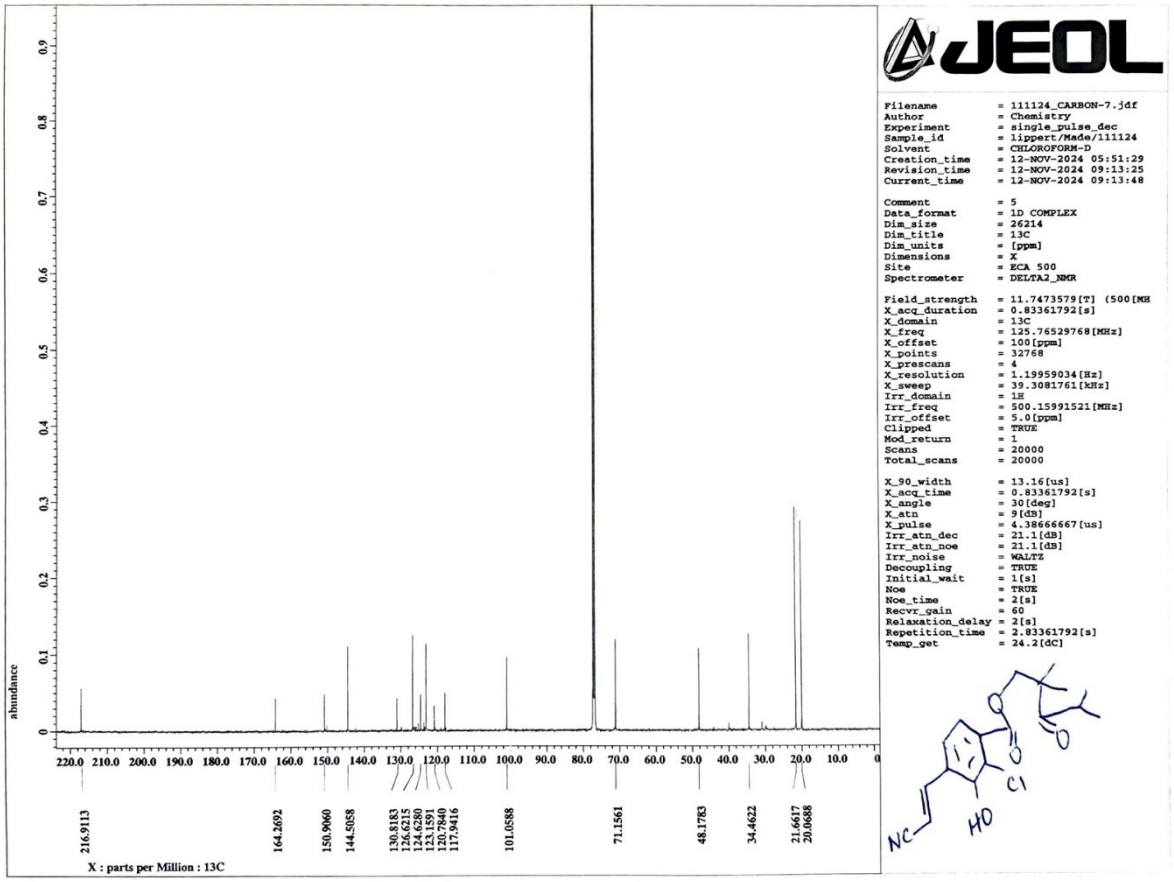

Figure S33: ^{13}C-NMR of compound **12** in $CDCl_3$.

[1] Adamson A. W., A Textbook of Physical Chemistry, Academic Press: New York, 1973.

[2] C. Reichardt, Solvents and Solvent Effects in Organic Chemistry, Third Edition, Wiley-VCH, Weinheim, Germany, (2003) 629.

[3] C. V. Stevani, S.M. Silva, W.J. Baader, Studies on the Mechanism of the Excitation Step in Peroxyoxalate Chemiluminescence, Eur. J. Org. Chem. (2000) 4037–4046.

[4] F.A. Augusto, G.A. De Souza, S.P. De Souza, M. Khalid, W.J. Baader, Efficiency of electron transfer initiated chemiluminescence, Photochem. Photobiol. 89 (2013) 1299–1317.

[5] I. Shimada, K. Maeno, Y. Kondoh, H. Kaku, K. Sugasawa, Y. Kimura, K. ichi Hatanaka, Y. Naitou, F. Wanibuchi, S. Sakamoto, S. ichi Tsukamoto, Synthesis and structure-activity relationships of a series of benzazepine derivatives as 5-HT2C receptor agonists, Bioorg. Med. Chem. 16 (2008) 3309–3320

[6] L.S. Ryan, J. Gerberich, J. Cao, W. An, B.A. Jenkins, R.P. Mason, A.R. Lippert, Kinetics-Based Measurement of Hypoxia in Living Cells and Animals Using an Acetoxymethyl Ester Chemiluminescent Probe, ACS Sens. 4 (2019) 1391–1398.

[7] M.J. Goodwin, J.C. Dickenson, A. Ripak, A.M. Deetz, J.S. McCarthy, G.J. Meyer, L. Troian-Gautier, Factors that Impact Photochemical Cage Escape Yields, Chem. Rev. 124 (2024) 7379–7464.

[8] W. Adam, I. Bronstein, A. V. Trofimov, R.F. Vasil'ev, Solvent-cage effect (viscosity dependence) as a diagnostic probe for the mechanism of the intramolecular chemically initiated electron-exchange luminescence (CIEEL) triggered from a spiroadamantyl-substituted dioxetane, J. Am. Chem. Soc. 121 (1999) 958–961.

[9] E.L. Bastos, S.M. Da Silva, W.J. Baader, Solvent cage effects: Basis of a general mechanism for efficient chemiluminescence, J. Org. Chem. 78 (2013) 4432–4439.

[10] M.A. Haidekker, E.A. Theodorakis, Environment-sensitive behavior of fluorescent molecular rotors, J. Biol. Eng. 4 (2010).

[11] M. Khalid, M.A. Oliveira, S.P. Souza, L.F.M.L. Ciscato, F.H. Bartoloni, W.J. Baader, Efficiency of intermolecular chemiluminescence systems lacks significant solvent cavity effect in binary toluene/diphenylmethane mixtures, J. Photochem. Photobiol. A: Chem. 312 (2015) 81–87.

[12] J. Da Chai, M. Head-Gordon, Long-range corrected hybrid density functionals with damped atom-atom dispersion corrections, Physical Chemistry Chemical Physics 10 (2008).

[13] R. Krishnan, J.S. Binkley, R. Seeger, J.A. Pople, Self-consistent molecular orbital methods. XX. A basis set for correlated wave functions, J. Chem. Phys. 72 (1980).

[14] M. J.Frisch, G. W.Trucks, H. B.Schlegel, G. E.Scuseria, M. A.Robb, J. R.Cheeseman, G.Scalmani, V.Barone, G. A.Petersson, H.Nakatsuji, X.Li, M.Caricato, A. V.Marenich, J.Bloino, B. G.Janesko, R.Gomperts, B.Mennucci, H. P.Hratchian, J. V.Ortiz, A. F.Izmaylov, J. L.Sonnenberg, D.Williams-Young, F.Ding, F.Lipparini, F.Egidi, J.Goings, B.Peng, A.Petrone, T.Henderson, D.Ranasinghe, V. G.Zakrzewski, J.Gao, N.Rega, G.Zheng, M. H. W.Liang, M.Ehara, K.Toyota, R.Fukuda, J.Hasegawa, M.Ishida, T.Nakajima, Y.Honda, O.Kitao, H.Nakai, T.Vreven, K.Throssell, J. A.Montgomery, J. E. P.Jr., F.Ogliaro, M. J.Bearpark, J. J.Heyd, E. N.Brothers, K. N.Kudin, V. N.Staroverov, T. A.Keith, R.Kobayashi, J.Normand, K.Raghavachari, A. P.Rendell, J. C.Burant, S. S.Iyengar, J.Tomasi, J. M. M. M.Cossi, M.Klene, C.Adamo, R.Cammi, J. W.Ochterski, R. L.Martin, K.Morokuma, O.Farkas, J. B.Foresman and D. J.Fox, Gaussian 16, revision A. 03, Wallingford CT, 2016.